On the identification of piecewise constant coefficients in optical diffusion tomography by level set

J. P. Agnelli [†] A. De Cezaro[‡] A. Leitão[§] M. Marques Alves [¶]

April 15, 2015

Abstract

In this paper, we propose a level set regularization approach combined with a split strategy for simultaneous identification of piecewise constant diffusion and absorption coefficients from a finite set of optical tomography data (Neumann-to-Dirichlet data). This problem is a high nonlinear inverse problem combining together the exponential and mildly ill-posedness of diffusion and absorption coefficients, respectively. We prove that the parameters-to-measurement map satisfies sufficient conditions (continuity in the L^1-topology) to guarantee regularization properties of the proposed level set approach. On the other hand, numerical tests considering different configurations bring new ideas on how to propose a convergent split strategy for the simultaneous identification of the coefficients. Therefore, the proposed numerical algorithm is stable and convergent as shows in the presented examples as well as it saves computational effort.

2000 Mathematics Subject Classification: 49N45, 65N21, 74J25.

Key words: Optical Tomography, Parameters Simultaneous Identification, Level Sets Regularization, Numerical Strategy .

1 Introduction

Optical tomography has demonstrated to be a powerful tool to obtain relevant physiologically information of tissues in a non-invasive manner. This puts optical tomography modalities very popular and with a large range of application in medial images. See [1, 17] and references therein for details.

[†]FaMAF-CIEM, Universidad Nacional de Córdoba, Medina Allende s/n 5000, Córdoba, Argentina. (agnelli@famaf.unc.edu.ar).

[‡]Institute of Mathematics Statistics and Physics, Federal University of Rio Grande, Av. Italia km 8, 96201-900 Rio Grande, Brazil (dcezaromtm@gmail.com).

[§]Department of Mathematics, Federal University of St. Catarina, P.O. Box 476, 88040-900 Florianópolis, Brazil (aleitao@mtm.ufsc.br).

[¶]Department of Mathematics, Federal University of St. Catarina, 88040-900 Florianópolis, Brazil (maicon.alves@ufsc.br).

There are many different approaches to modeling the physics of light propagation in a medium, e.g. [1, 17] and references therein. In this contribution we are interested in the so called diffusion optical tomography (DOT). In other words, the DOT regime assumes visible (or near infrared) light in the predefined wavelength to probe highly scattering medium. The aim of DOT is to obtain quantitative information on optical properties of an object embedded in the medium. For a complete overview on optical tomography modalities the reader can consult the topical review [1, 17] and references therein.

A simple physical formulation of DOT, where light propagation is modeled by a diffusion approximation and the excitation frequency is set to zero, is governed by the following boundary value problem

$$-\nabla \cdot (a(x)\nabla u) + c(x)u = 0 \quad \text{in } \Omega \tag{1}$$

$$a(x)\partial_\nu u = g \quad \text{on } \Gamma\,, \tag{2}$$

where $\Omega \subset \mathbb{R}^N$, $N \in \{2, 3, 4\}$, is open, bounded and connected with boundary Γ Lipschitz; the diffusion and absorption coefficients $a(x)$ and $c(x)$, respectively, are measurable real-valued functions and ν is the outer normal to the boundary of Ω, that we denote by Γ. Moreover, $g \in H^{-1/2}(\Gamma)$ is the Neumann boundary data.

Although most of the physiological information is contained in the absorption coefficient, the scattering coefficient in tissue is, in general, considerably larger. It is well known that the presence of unknown scatter can lead to artifacts and false structure in the reconstruction of the absorption properties of the medium [1, 17]. Hence, the problem of interest in DOT is the simultaneous identification of absorption and the scattering properties.

Since the absorbed and scattered characteristic of the medium are unique determined by the pair of coefficients (a, c) in (1)-(2) (see [1, 17]), in this contribution, we proposed an level set regularization approach [15, 10, 7, 8] coupling with a split strategy for stable simultaneous identification of the location and the shape of piecewise constant real-valued diffusion $a(x)$ and absorption $c(x)$ coefficients in (1)–(2), from the knowledge of a finite set of available measurements of the potential $h := u|_\Gamma$, corresponding to the current profiles $g \in H^{-1/2}(\Gamma)$ in (2).

Related works: In [21], a Levenberg–Marquardt method for recovering internal boundaries of piecewise constant coefficients of an elliptic PDE as (1) was implemented. The proposed method is based on the series expansion approximation of the smooth boundaries and on the finite element method. However, in [21], there is not a theoretical result that guarantees regularizing properties of the iterated approximated solution. Indeed, as far as the authors are aware, there is not theoretical regularization approaches in the literature for recovering the pair of coefficients (a, c) in (1) for data in the boundary.

In [27], the authors did a carefully designed experiment aimed to provide solid evidence that both absorption and scattering images of a heterogeneous scattering media can be reconstructed independently from diffusive optical tomography data. The author's also discuss the absorption scattering cross-talk issue.

Although, it is well known that the identification of a and c (simultaneously) is not possible in a general case, as is shown by Arridge and Lionheart in [2], recently, B. Harrach [18] obtained uniqueness results of simultaneous determination of a and c in (1)-(2) assuming that $a \geq a_0 > 0$ is

piecewise constant and $c \in L^\infty_+$ [1] is piecewise analytic, from the knowledge of all pairs of Newmann and Dirichlet boundary values $a\partial_\nu u|_{\tilde{\Gamma}}$ and $u|_{\tilde{\Gamma}}$, on an arbitrarily small open part $\tilde{\Gamma}$ of the boundary Γ. The differences between B. Harrach [18] results and our approach is that we are considering a more practical approach: we have access only to a finite number Newmann-Dirichlet pairs.

We also remark that the now well known QPAT (quantitative photo-acoustic tomography) problem, in the diffusive approach, also aims to simultaneous recover (a, c) in an elliptic boundary valued problem. See for example [25] and references therein. However, in the QPAT situation the solution of the "first inverse problem" generate internal data for the reconstruction. In this sense, the QPAT problem is very different to the identification problem that we are facing here.

Novelties: The novelties of this contribution are divided as follows:

- We prove the continuity of the parameter-to-measurement (forward) map F (as defined in (3)) in the $L^1(\Omega)$-topology. It is done in Theorem 3 in Section 2. This is possible thanks to a generalization of Meyer's theorem [22] for the regularity of the solution of (1)-(2) in $W^{1,p}(\Omega)$, for some $p > 2$ (see Theorem 1). The generalization of Meyer's theorem for the equations (1)-(2) is presented in details in the Appendix 7.

  In Section 3, we introduce a level set approach. In contrast to the seminal approach of Santosa in [24] on level set for inverse problems, our approach consists in a parametrization of the non-smooth admissible set of parameters with a pair of $H^1(\Omega)$ functions concatenated with a restriction of the search space using nonlinear constraints. Such approach allows us to enforce the desired additional properties on the pair of parameters (a, c) (namely: (a, c) is a piecewise constant pair of function, describing the high diffusion and absorption contrast between the optical properties of the object) that are not smooth.

  Given the continuity of F in the $L^1(\Omega)$-topology, it is now a standard result to prove that the level set approach is a regularization method as in the classical theory of regularization [13], e.g. [7, 8, 11, 10]. Therefore, we only point out the convergence and stability results without a formal proof in Subsection 3.2.

- Another improvement of the proposed level-set approach is related to the numerical implementation in Section 5. It is worth to remind the reader that we aim to simultaneous reconstruct the pair (a, c) of piecewise constant functions from a finite set of optical measurements. With this aim, we first run several numerical experiments in order to recover the absorption coefficient c, based on either total or partial knowledge of a. From this experiments we saw that the level set method for identifying c^* performs well, even if a good approximation for a^* is not known. This is presented in Subsection 5.1. After that, in Subsection 5.2 we run another set of experiments but know concerning the identification of the diffusion coefficient a, based on either total or partial knowledge of c. In this case, we saw that the level set method for identifying a^* performs well if a good approximation for c^* is available, but may generate a sequence a_k that does not approximate a^* if the initial guess for the coefficient c is far from c^*. Such features of the identification problems suggests one of the main results in the

[1] The subscript $'+'$ denotes positive essential infima.

numerical perspective presented in Subsection 5.3. Given the initial guess (a_0, c_0), we adopted the strategy to freeze the coefficient $a_k = a_0$ during the first iterations, and to iterate the algorithm only w.r.t to the coefficient c. We follow this strategy until the iterated sequence c_k stagnates. Then, we freeze" the absorption coefficient $c = c_k$ and iterate the algorithm w.r.t. a after stagnation of the iteration. Finally, iterate both simultaneously. This numerical strategy gives very good results and save computational effort as well.

We ended this contribution in Section 6 with some conclusions and further developments.

General Notation. We denote by $\mathbb{R}^N$, $N \geq 2$, the N-dimensional Euclidean space endowed the usual scalar product $x \cdot y = \sum_{i=1}^N x_i y_i$ and norm $|x| = \sqrt{x \cdot x}$, where $x = (x_i)_{i=1}^N$ and $y = (y_i)_{i=1}^N$. Given two normed vector spaces $(\mathcal{X}, \|\cdot\|_{\mathcal{X}})$ and $(\mathcal{Y}, \|\cdot\|_{\mathcal{Y}})$ we always consider the product space $\mathcal{X} \times \mathcal{Y}$ enwowed with the product topology generated by the norm $\|(x, y)\| := \|x\| + \|y\|$ (or the equivalent norms $(\|x\|^2 + \|y\|^2)^{1/2}$ or $\max\{\|x\|, \|y\|\}$), where $(x, y) \in \mathcal{X} \times \mathcal{Y}$. We also use the short notation $\mathcal{X}^2 = \mathcal{X} \times \mathcal{X}$.

2 The Parameter to Measurement Map

We start this section by assuming that $a(x)$ is known for all $x \in \Gamma$. Then, for each input current profile $g \in H^{-1/2}(\Gamma)$ in (1)-(2), we define parameter-to-measurement (forward) map

$$\begin{array}{rcl} F := F_g : D(F) \subset L^1(\Omega) \times L^1(\Omega) & \to & H^{1/2}(\Gamma) \\ (a, c) & \mapsto & h := u|_\Gamma, \end{array} \tag{3}$$

where $u = u(g)$ is the unique corresponding solution of (1)-(2), for the parameter space $D(F)$ defined as:

Definition 1. *Denote by $D(F)$ the set of pairs of $L^1(\Omega)$ functions (a, c) on Ω satisfying the following condition:*

$$0 < \underline{a} \leq a(x) \leq \overline{a}, \quad 0 < \underline{c} \leq c(x) \leq \overline{c} \quad \forall x \text{ a.e. in } \Omega, \tag{4}$$

where $\underline{a}, \underline{c}, \overline{a}$ and $\overline{c}$ are known positive real numbers such that $\underline{a} \leq \overline{a}$ and $\underline{c} \leq \overline{c}$.

We now make some comments about Definition 1 and the definition of the forward map F. First, it is easy to check that $D(F)$ is a convex subset of $[L^1(\Omega)]^2$. Second, the forward map F is well-defined because for each $(a, c) \in D(F)$ there exists a unique solution $u \in H^1(\Omega)$ of (1)–(2) (see e.g. [6]). Third, since $D(F)$ depends on the scalars $\underline{a}, \underline{c}, \overline{a}$ and $\overline{c}$, it turns out that F also depends on the latter scalars. However, we are assuming the scalars to be known, fixed and independent of each given current g. Fourth, we are not assuming any smoothness condition on the pair parameters $(a, c) \in D(F)$. In particular the latter fact allow us to consider solutions of (1)–(2) corresponding to piecewise constant coefficients.

This section is devoted to prove the continuity of the forward map F in the $L^1(\Omega)$ - topology. In order to make such proof easy to understand we will consider the parameter-to-*solution* map G_g

defined as

$$G := G_g \,:\, D(F) \subset [L^1(\Omega)]^2 \longrightarrow H^1(\Omega)$$
$$(a,c) \longmapsto G_g(a,c) := u(g)\,, \tag{5}$$

where $u(g) \in H^1(\Omega)$ is the (unique) solution of (1)–(2) for each input data $g \in H^{-1/2}(\Gamma)$ and parameters $(a,c) \in D(F)$ (see [6]). Moreover, we will uses the following well know result: any weak solution $u = u(g) \in H^1(\Omega)$ of (1)–(2) satisfies the (weak) formulation (see [6])

$$\int_\Omega a\nabla u \cdot \nabla\varphi dx + \int_\Omega cu\varphi dx = \int_\Gamma g\varphi dS \quad \forall \varphi \in H^1(\Omega). \tag{6}$$

Remark 1. *Given the definition of the forward map F in (3), its turns out that it can be written as*

$$F = \gamma_0 \circ G, \tag{7}$$

where $\gamma_0 : H^1(\Omega) \to H^{1/2}(\Gamma)$ is the trace operator of order zero [6]. Since the trace operator γ_0 is linear and continuous [6], it follows that the continuity of F follows from the continuity of G.

In order to prove the continuity of the operator G defined in (5) in the desired topology, we will use a generalization of Meyer's theorem [16] on the regularity of the solution of (1) - (2). Since the proof follows the general lines of presented in [16], we will show the main differences in the Appendix.

Theorem 1 (Meyer's theorem generalized)**.** *Let $\Omega \subset \mathbb{R}^N$, $N \in \{2,3,4\}$, be a connected bounded open set with a Lipschitz boundary Γ and let $(a,c) \in D(F)$. Then, there exists a real number $p_M > 2$ depending only on Ω, $\underline{a}$ and $\overline{a}$) such that the following condition hold for every $p \in (2, p_M)$: If $g \in W^{1-(1/q),q}(\Gamma)'$, where $q := p/(p-1)$, then the unique solution u of (1)– (2) belongs to $W^{1,p}(\Omega)$.*

Next we will present a lemma that is used in the main theorem of this section.

Lemma 2. *Let $h(x)$ be a measurable function such that $M \geq |h(x)|$ for all x a.e. in Ω, for some constant $M > 0$. Then, $h \in L^s(\Omega)$ for all $1 \leq s < \infty$ and*

$$\|h\|_{L^s(\Omega)} \leq M^{(s-1)/s} \|h\|^{1/s}_{L^1(\Omega)}.$$

Proof. Note that

$$\|h\|^s_{L^s(\Omega)} = \int_\Omega |h(x)||h(x)|^{s-1} dx \leq M^{s-1} \|h\|_{L^1(\Omega)},$$

which readily implies the desired result. □

In the next theorem we will prove the continuity of the forward map F in the $[L^1(\Omega)]^2$ topology. The latter result, will follow as a direct consequence of the continuity of the operator G defined in (5).

Theorem 3. *Let $p \in (2, p_M)$, where $p_M > 2$ is given by Theorem 1, and let $q := p/(p-1)$. Then, for any $g \in W^{1-(1/q),q}(\Gamma)'$ the operator G_g defined in (5) is continuous (in the $[L^1(\Omega)]^2$ topology).*

As a consequence, for any $g \in W^{1-(1/q),q}(\Gamma)'$, the forward map F defined in (3) is also continuous in the $[L^1(\Omega)]^2$ topology.

Proof. Let $g \in W^{1-(1/q),q}(\Gamma)'$ and consider the corresponding solutions $u' = u(a', c')$ and $u = u(a, c)$ of (1)–(2) with parameters $(a', c'), (a, c) \in D(F)$, respectively.

Since (a', c', u') and (a, c, u) satisfy the identity (6) for all $\varphi \in H^1(\Omega)$ we have

$$\int_\Omega (a\nabla u - a'\nabla u') \cdot \nabla\varphi dx + \int_\Omega (cu - c'u')\varphi dx = 0\,. \tag{8}$$

Defining $w := u - u' \in H^1(\Omega)$ and using (8) with $\varphi = w$ we obtain (after some algebraic manipulations)

$$\int_\Omega [a - a']\nabla u' \cdot \nabla w dx + \int_\Omega a\nabla w \cdot \nabla w dx + \int_\Omega [c - c']u' w dx + \int_\Omega cww dx = 0,$$

which in turn is equivalent to

$$\int_\Omega a(x)|\nabla w|^2 dx + \int_\Omega c(x)|w|^2 dx = \int_\Omega [a' - a]\nabla u' \cdot \nabla w dx + \int_\Omega [c' - c]u' w dx. \tag{9}$$

In view of Theorem 1 (for $a'(x)$ and $c'(x)$) we have $u' \in W^{1,p}(\Omega)$. Thus, defining $s := 2p/(p-2)$, it follows from (9), (4), Lemma 2 and the Holder inequality (note that $1/s + 1/p + 1/2 = 1$) that

$$\begin{aligned}
\min\{\underline{a}, \underline{c}\}\|w\|^2_{H^1} &\le \|a' - a\|_{L^s}\|\nabla u'\|_p\|\nabla w\|_2 + \|c' - c\|_{L^s}\|u'\|_{L^p}\|w\|_{L^2} \\
&\le \left(\|a' - a\|_{L^s}\|\nabla u'\|_p + \|c' - c\|_{L^s}\|u'\|_{L^p}\right)\|w\|_{H^1} \\
&\le 2\max\{\overline{a}, \overline{c}\}\Big)^{(s-1)/s}\|u'\|_{W^{1,p}}\left(\|a' - a\|_{L^1} + \|c' - c\|_{L^1}\right)^{1/s}\|w\|_{H^1}.
\end{aligned}$$

The latter inequality combined with the facts that $G_g(a', c') = u'$, $G_g(a, c) = u$ (see (5)) and $w = u - u'$ gives

$$\|G_g(a, c) - G_g(a', c')\|_{H^1} \le M\|u'\|_{W^{1,p}}\left(\|a - a'\|_{L^1} + \|c - c'\|_{L^1}\right)^{1/s}, \tag{10}$$

which proves the continuity of G_g in the $L^1(\Omega)$ topology, where $M := \dfrac{2\max\{\overline{a}, \overline{c}\}\Big)^{(s-1)/s}}{\min\{\underline{a}, \underline{c}\}}$. The last statement of the theorem now follows easily from the first one and Remark 1. □

We now make a few comments about Theorem 3. First, according to Theorem 1, the real number $p_M > 2$ depends on Ω and, in the present setting, on $\underline{a}, \underline{c}, \overline{a}$ and $\overline{c}$. Second, since $q < 2$, it follows that $W^{1-(1/q),q}(\Gamma)' \subset H^{-1/2}(\Gamma)$. As a consequence of the latter inclusion, we have that the condition on g that appeared on Theorem 3 is stronger that the usual inclusion $g \in H^{-1/2}(\Gamma)$. Third, condition (10) gives that both operators G and F are (locally) Holder continuous in the $L^1(\Omega)$ topology.

3 The level set framework with a finite number of experiments

It is already known that in diffusive optical tomography the full Neumann-to-Dirichlet map (equivalently, the boundary data h at Γ corresponding to the $a\frac{\partial u}{\partial \nu}$) are required to obtain uniqueness of the parameters (a, c) in (1)-(2)(see [18]). However, in real applications, only a finite number of observations/measurements are available. Therefore, we are strongly invited to make a quantity ℓ of well-placed experiments in order to obtain reconstructions of acceptable quality. In other words, the inverse problem that we are shall to deal with consists in identification of the pair of coefficients (a, c) from a finite number ℓ of experiments, where the inputs $g_m := a\frac{\partial u_m}{\partial \nu}(x)$ are chosen in an appropriate way such that the corresponding measurements $u_m(x) = h_m$ for $x \in \Gamma$, are available, for $m = 1, \cdots, \ell$. As before, the corresponding potential u_m satisfies

$$\begin{aligned} \nabla \cdot (a\nabla u_m) + cu_m = 0\,, \qquad & \text{in } \Omega\,, \quad m = 1, \cdots, \ell\,, \\ a\frac{\partial u_m}{\partial \nu}(x) = g_m \qquad & \text{at } \Gamma. \end{aligned} \tag{11}$$

This problem is known in the literature as the inverse problem for the Neumann-to-Dirichlet operator with a finite number of experiments. In this context, the identification problem can be written in terms of the system of nonlinear equations

$$F_m(a, c) = h_m\,, \qquad m = 1, \cdots, \ell\,, \tag{12}$$

where $F_m := F_{g_m}$ is defined as in (3), for each $m \in \{1, \cdots, \ell\}$.

Moreover, given the nature of the measurements, we can not expect that exact data $h_m \in H^{1/2}(\Gamma)$ are available. Instead, one disposes only an approximate measured data $h_m^\delta \in L^2(\Gamma)$ satisfying

$$\left\| h_m^\delta - h_m \right\|_{L^2(\Gamma)} \leq \delta\,, \quad \text{for } m = 1, \cdots, \ell \tag{13}$$

where $\delta > 0$ is the noise level.

Remark 2. *From Theorem 3, we know that each forward map F_m in (12) is continuous in the L^1-topology.*

3.1 Modeling the parameter space: The level set framework

In contrast with the previous section, now we assume that the pair of parameter (a, c) are piecewise constant function assuming two distinct values, i.e. $a(x) \in \{a^1, a^2\}$ and $c(x) \in \{c^1, c^2\}$ a.e. in $\Omega \subset \mathbb{R}^N$, but, still $(a(x), c(x)) \in D(F)$. Hence, one can assume the existence of open and mensurable sets $\mathbb{A}_1 \subset\subset \Omega$ and $\mathbb{C}_1 \subset\subset \Omega$, with $\mathcal{H}^1(\partial\mathbb{A}_1) < \infty$ and $\mathcal{H}^1(\partial\mathbb{C}_1) < \infty$,[2] s.t. $a(x) = a^1\,, x \in \mathbb{A}_1$, $c(x) = c^1\,, x \in \mathbb{C}_1$ and $a(x) = a^2\,, x \in \mathbb{A}_2 := \Omega - \mathbb{A}_1$, $c(x) = c^2\,, x \in \mathbb{C}_2 := \Omega - \mathbb{C}_1$.

Consequently, with the assumption that the conductivity and the absorption coefficients are piecewise constant, the pair of parameter distribution in (1)–(2) can be modeled as

$$(a(x), c(x)) = (a^2 + (a^1 - a^2)\chi_{\mathbb{A}_1}(x), c^2 + (c^1 - c^2)\chi_{\mathbb{C}_1}(x))\,, \tag{14}$$

where χ_S is the indicator function of the set S.

[2]Here $\mathcal{H}^1(S)$ denotes the one-dimensional Hausdorff-measure of the set S.

Level set framework: In order to model the space of admissible parameters (the pair of piecewise constant function (a, c), we use a standard level set (sls) approach proposed in [15, 9, 7, 8, 10]. We remark that many other level set approaches are known in the literature, e.g., [11, 10, 9, 7, 12, 5, 21, 28, 26]. In particular, the analysis of level set approach for the pair of parameter that have many piecewise components follows essentially from the techniques derived in [8]. Finally, if a^j, c^j are assuming unknown then one can use the ideas of the level set approach in [7] to recover the levels values as well. Recently in [9, 10, 11], piecewise constant level set approaches (PCLS) were derived for identification of piecewise parameters. The (PCLS) approach consists in introducing constraints in the admissible level set function s.t. it becomes piecewise constant. In the (PCLS) approaches, we do not need to introduce the Heaviside projections H (see below) to model the parameter space. However, the introductions of constraints imply in other difficulties in the level set regularization analysis [9, 10]. Advantages and disadvantages of (sls) and (PCLS) approaches were discussed in [9, 10].

According to the (sls) representation strategy, level set functions $\phi_a, \phi_c : \Omega \to \mathbb{R}$, in $H^1(\Omega)$, are chosen in such a way that its zero level-set $\Gamma_{\phi_a} := \{x \in \Omega\,;\ \phi_a(x) = 0\}$ and $\Gamma_{\phi_c} := \{x \in \Omega\,;\ \phi_c(x) = 0\}$ defines connected curves within Ω and that the discontinuities of the parameters are located 'along' Γ_{ϕ_a} and Γ_{ϕ_c}, respectively.

Introducing the Heaviside projector

$$H(t) \ := \ \begin{cases} 1, & \text{if } t > 0 \\ 0, & \text{if } t \leq 0 \end{cases},$$

the conductivity/absorption parameter distribution $(a(x), c(x))$ is represented in the form

$$(a(x), c(x)) \ = \ (a^1 H(\phi_a) + a^2(1 - H(\phi_a)), c^1 H(\phi_c) + c^2(1 - H(\phi_c))) \ =: \ P(\phi_a, \phi_c)\,. \tag{15}$$

Notice that $(a(x), c(x)) = (a^i, c^j)$, $x \in \mathbb{A}_i \cap \mathbb{C}_j$ for $i, j \in \{1, 2\}$, where the sets $\mathbb{A}_i$ and $\mathbb{C}_j$ are defined by $\mathbb{A}_1 = \{x \in \Omega\,;\ \phi_a(x) \geq 0\}$, $\mathbb{A}_2 = \{x \in \Omega\,;\ \phi_a(x) < 0\}$, $\mathbb{C}_1 = \{x \in \Omega\,;\ \phi_c(x) \geq 0\}$ and $\mathbb{C}_2 = \{x \in \Omega\,;\ \phi_c(x) < 0\}$. Thus, the operator P establishes a straightforward relation between the level sets of ϕ_a and ϕ_c and the sets $\mathbb{A}_i$ and $\mathbb{C}_j$ representing our *a priori* knowledge about the solution (a, c).

As already observed in [8], the operator H maps $H^1(\Omega)$ into the space

$$\mathcal{V}_{0,1} \ := \ \{z \in L^\infty(\Omega)\,|\,z = \chi_S\,,\ S \subset \Omega \text{ measurable, } \mathcal{H}^1(\partial S) < \infty\}\,. \tag{16}$$

Therefore, the operator P in (15) maps $H^1(\Omega) \times H^1(\Omega)$ into the admissible class $\mathcal{V}$ defined by

$$\mathcal{V} \ := \ \{(z_1, z_2) \in (L^\infty(\Omega))^2\,|\,(z_1, z_2) := (a_1 + (a_2 - a_1)\,\chi_{\mathbb{A}_1}, c_1 + (c_2 - c_1)\,\chi_{\mathbb{C}_1})\,,\ \mathbb{A}_1, \mathbb{C}_1 \subset \Omega\}\,. \tag{17}$$

Within this framework, the inverse problem in (12), with data given as in (13), can be written in the form of the system of operator equation

$$F_m(P(\phi_a, \phi_c)) \ = \ h_m^\delta \qquad m = 1, \cdots, \ell. \tag{18}$$

Let we make the following general assumption

(A1) Equation (18) has a solution, i.e. there exists $(a^*, c^*) \in L^\infty(\Omega) \times L^\infty(\Omega)$ satisfying $F((a^*, c^*)) = h$; there exists a pair of function $({\phi_a}^*, {\phi_c}^*) \in [H^1(\Omega)]^2$ satisfying $|\nabla {\phi_a}^*| \neq 0$ and $|\nabla {\phi_c}^*| \neq 0$, in a neighborhood of $\{{\phi_a}^* = 0\}$ and $\{{\phi_c}^* = 0\}$ such that $H({\phi_a}^*) = z_a \in L^\infty(\Omega)$, $H({\phi_c}^*) = z_c \in L^\infty(\Omega)$ such that $P(z_a, z_c) = (a^*, c^*)$.

Since an approximate solution (ϕ_a, ϕ_c) of (18) is calculated, a corresponding approximate solution of (12) is obtained in a straightforward way: $(a, c) = P(\phi_a, \phi_c)$.

3.2 Leve set regularization

Since the unknown coefficients (a, c) are piecewise constant function, a natural alternative to obtain stable solutions of the operator equation (12) is to use a least-square approach combined with a total variation regularization. This corresponds to a Tikhonov-type regularization [7, 8, 10]. Within the level-set framework presented aboveHowever, in real applications, only a finite number of observations/measurements are available, the Tikhonov-type regularization approach for obtaining a regularized solution to the operator equation (18) is based on the minimization of the energy functional

$$\mathcal{F}_\alpha(\phi_a, \phi_c) := \sum_{m=1}^{N} \|F_m(P(\phi_a, \phi_c)) - h_m^\delta\|_Y^2 + \alpha R(\phi_a, \phi_c)\,, \tag{19}$$

where

$$R(\phi_a, \phi_c) = \left(|H(\phi_a)|_{\mathtt{BV}(\Omega)} + |H(\phi_c)|_{\mathtt{BV}(\Omega)} + \|\phi_a - \phi_{a0}\|_{H^1(\Omega)}^2 + \|\phi_c - \phi_{c0}\|_{H^1(\Omega)}^2\right)$$

and $\alpha > 0$ plays the role of a regularization parameter. This approach is based on TV-H^1 penalization. The H^1–terms act simultaneously as a control on the size of the norm of the level set function and as a regularization on the space $H^1(\Omega)$. The $\mathtt{BV}(\Omega)$-seminorm terms are well known for penalizing the length of the Hausdorff measure of the boundary of the sets $\{x \in \Omega : \phi_a(x) > 0\}$, $\{x \in \Omega : \phi_c(x) > 0\}$ (see [14]).

In general, variational minimization techniques involve compact embedding arguments on the set of admissible minimizers and continuity of the operator in such set to guarantee the existence of minimizers. The Tikhonov functional in (19) does not allow such characteristic, since the Heaviside operator H and consequently the operator P are discontinuous. Therefore, given a minimizing sequence (ϕ_a^k, ϕ_c^k) for $\mathcal{F}_\alpha$ we cannot prove existence of a (weak-*) convergent subsequence. Consequently, we cannot guarantee the existence of a minimizer in $[H^1(\Omega)]^2 \times \mathbb{R}^2$. In other words, the graph of $\mathcal{F}_\alpha$ is not closed in the desired topology.

To overcome this difficulty in [15, 7, 8] was introduced the concept of generalized minimizers were the graph $\mathcal{F}_\alpha$ becomes closed. It allow us to guarantee the existence of minimizers of the Tikhonov functional (19). For sake of completeness, we present the concept of generalized minimizers below.

The concept of generalized minimizers: For each $\varepsilon > 0$, we define the smooth approximation to H given by:

$$H_\varepsilon(t) := \begin{cases} 1 + t/\varepsilon & \text{for } \ t \in [-\varepsilon, 0] \\ H(t) & \text{for } \ t \in \mathbb{R}/\,[-\varepsilon, 0] \end{cases}$$

and the corresponding operator

$$P_\varepsilon(\phi_a, \phi_c) \ := \ (a^1 H_\varepsilon(\phi_a) + a^2(1 - H_\varepsilon(\phi_a)), c^1 H_\varepsilon(\phi_c) + c^2(1 - H_\varepsilon(\phi_c)))\,. \tag{20}$$

Definition 2. *Let the operators H, P, H_ε and P_ε be defined as above.*
a) A **vector** $(z_1, z_2, \phi_a, \phi_c) \in [L_\infty(\Omega)]^2 \times [H^1(\Omega)]^2$ *is called* **admissible** *when there exists sequences* $\{\phi_a^k\}$ *and* $\{\phi_c^k\}$ *of* $H^1(\Omega)$*-functions satisfying*

$$\lim_{k\to\infty} \|\phi_a^k - \phi_a\|_{L^2(\Omega)} = 0\,, \quad \lim_{k\to\infty} \|\phi_c^k - \phi_c\|_{L^2(\Omega)} = 0$$

and there exists a sequence $\{\varepsilon_k\} \in \mathbb{R}^+$ *converging to zero such that*

$$\lim_{k\to\infty} \|H_{\varepsilon_k}(\phi_a^k) - z_1\|_{L^1(\Omega)} = 0 \;\; \textit{and} \;\; \lim_{k\to\infty} \|H_{\varepsilon_k}(\phi_c^k) - z_2\|_{L^1(\Omega)} = 0\,.$$

b) A **generalized minimizer** *of the Tikhonov functional $\mathcal{F}_\alpha$ in (19) is considered to be any admissible vector $(z_1, z_2, \phi_a, \phi_c)$ minimizing*

$$\mathcal{G}_\alpha(z_1, z_1, \phi_a, \phi_c) := \sum_{m=1}^{N} \|F_m(Q(z_1, z_2)) - h_m^\delta\|^2_{H^{1/2}(\Omega)} + \alpha R(z_1, z_2, \phi_a, \phi_c) \tag{21}$$

over the set of admissible vectors, where

$$Q : [L_\infty(\Omega)]^2 \times \mathbb{R}^2 \ni (z_1, z_2) \mapsto (a^1 z_1 + a^2(1 - z_2), c^1 z_2 + c^2(1 - z_2)) \in [L_\infty(\Omega)]^2\,,$$

and the functional R is defined by

$$R(z_1, z_2, \phi_a, \phi_c) \;\; := \;\; \rho(z_1, z_2, \phi_a, \phi_c)\,, \tag{22}$$

with

$$\rho(z_1, z_2, \phi_a, \phi_c) := \inf\left\{\liminf_{k\to\infty}\left(|H_{\varepsilon_k}(\phi_a^k)|_{\mathtt{BV}(\Omega)} + |H_{\varepsilon_k}(\phi_c^k)|_{\mathtt{BV}(\Omega)} + \|\phi_a - \phi_{a0}\|^2_{H^1(\Omega)} + \|\phi_{ck} - \phi_{c0}\|^2_{H^1(\Omega)}\right)\right\}. \tag{23}$$

Here the infimum is taken over all sequences $\{\varepsilon_k\}$ and $\{\phi_a^k, \phi_c^k\}$ characterizing $(z_1, z_2, \phi_a, \phi_c)$ as an admissible vector.

3.3 Convergence analysis of the level set approach

In this subsection we present the regularization properties of the proposed level set approach to the inverse problem of identifying (a, c) in the diffusive optical tomography model (1)–(2). Since the resutls follows straightforward arguments presented before in [7, 8, 10] we do not strave in presenting the proves.

Theorem 4. *The following assertions hold true.*
i) The functional $\mathcal{G}_\alpha$ in (19) attains minimizers on the set of admissible vectors.
ii) [**Convergence for exact data**] *Assume that we have exact data, i.e. $h^\delta = h$. For every $\alpha > 0$ denote by $(z_\alpha^1, z_\alpha^2, \phi_{a\alpha}, \phi_{c\alpha})$ a minimizer of $\mathcal{G}_\alpha$ on the set of admissible vectors. Then, for every sequence of positive numbers $\{\alpha_k\}$ converging to zero there exists a subsequence, denoted again by $\{\alpha_k\}$, such that $(z_{\alpha_k}^1, z_{\alpha_k}^2, \phi_{a\alpha_k}, \phi_{c\alpha_k})$ is strongly convergent in $L^1(\Omega) \times L^2(\Omega)$. Moreover, the limit is a solution of (18).*

iii) **[Convergence for noise data]** *Let $\alpha = \alpha(\delta)$ be a function satisfying $\lim_{\delta\to 0}\alpha(\delta) = 0$ and $\lim_{\delta\to 0}\delta^2\alpha(\delta)^{-1} = 0$. Moreover, let $\{\delta_k\}$ be a sequence of positive numbers converging to zero and $\{h^{\delta_k}\} \in H^{1/2}(\partial\Omega)$ be corresponding noise data satisfying (13). Then, there exists a subsequence, denoted again by $\{\delta_k\}$, and a sequence $\{\alpha_k := \alpha(\delta_k)\}$ such that $(z^1_{\alpha_k}, z^2_{\alpha_k}, \phi_{a\alpha_k}, \phi_{c\alpha_k})$ converges in $[L^1(\Omega)]^2 \times [L^2(\Omega)]^2$ to solution of (18).*

Proof. The proof follows straightforward the arguments in [8], Theorem 6, Theorem 8 and Theorem 9, respectively and therefore will be omitted. □

4 Numerical realization

In this section we introduce the functional $\mathcal{G}_{\varepsilon,\alpha}$, which can be used for the purpose of numerical implementations. This functional is defined in such a way that it's minimizers are 'close' to the generalized minimizers of $\mathcal{F}_\alpha$ in a sense that will be made clear later (see Proposition 5). For each $\varepsilon > 0$ we define the functional

$$\mathcal{G}_{\varepsilon,\alpha}(\phi_a, \phi_c) \ := \sum_{m=1}^{N} \|F_m(P_\varepsilon(\phi_a, \phi_c)) - h^\delta_m\|^2_Y + \alpha R_\varepsilon(\phi_a, \phi_c) \ , \tag{24}$$

where

$$R_\varepsilon(\phi_a, \phi_c) := \left(|H_\varepsilon(\phi_a)|_{\mathtt{BV}(\Omega)} + |H_{\varepsilon_k}(\phi_c)|_{\mathtt{BV}(\Omega)} + \|\phi_a - \phi_{a0}\|^2_{H^1(\Omega)} + \|\phi_c - \phi_{c0}\|^2_{H^1(\Omega)}\right) .$$

The next result guarantees that for $\varepsilon \to 0$ the functional $\mathcal{G}_{\varepsilon,\alpha}$ attain a minimizer. Moreover, the minimizers of $\mathcal{G}_{\varepsilon,\alpha}$ approximate a generalized minimizer of $\mathcal{F}_\alpha$.

Proposition 5.
i) Given α, $\varepsilon > 0$ and ϕ_{a0}, ϕ_{c0} in $H^1(\Omega)$, then the functional $\mathcal{G}_{\varepsilon,\alpha}$ in (24) attains a minimizer on $[H^1(\Omega)]^2 \times \mathbb{R}^2$.
ii) Let α, be given. For each $\varepsilon > 0$ denote by $(\phi_{a\varepsilon,\alpha}, \phi_{c\varepsilon,\alpha})$ a minimizer of $\mathcal{G}_{\varepsilon,\alpha}$. There exists a sequence of positive numbers $\{\varepsilon_k\}$ converging to zero such that $(H_{\varepsilon_k}(\phi_{a\varepsilon_k,\alpha}), H_{\varepsilon_k}(\phi_{c\varepsilon_k,\alpha}), \phi_{a\varepsilon_k,\alpha}, \phi_{c\varepsilon_k,\alpha})$ converges strongly in $[L^1(\Omega)]^2 \times [L_2(\Omega)]^2$ and the limit is a generalized minimizer of $\mathcal{F}_\alpha$ in the set of admissible vectors.

Proof. The proof follows the ideas in [8], Lemma 10 and Theorem 11 respectively. Therefore we will not present the details it in this paper. □

Proposition 5 justify the use functional $\mathcal{G}_{\varepsilon,\alpha}$ in order to obtain numerical approximations to the generalized minimizers of $\mathcal{F}_\alpha$. It is worth noticing that, differently from $\mathcal{F}_\alpha$, the minimizers of $\mathcal{G}_{\varepsilon,\alpha}$ can be actually computed. In the next subsection we compute the first order conditions of optimality for the functional $\mathcal{G}_{\varepsilon,\alpha}$, which will allow us to compute the desired minimizers.

4.1 Optimality conditions for the Tikhonov functional $\mathcal{G}_{\varepsilon,\alpha}$

For the numerical purposes we have in mind, it is necessary to derive the first order optimality conditions for a minimizer of the functionals $\mathcal{G}_{\varepsilon,\alpha}$. To this end we consider $\mathcal{G}_{\varepsilon,\alpha}$ in (24) and we look

for the Gâteaux directional derivatives with respect to ϕ_a, ϕ_c. For simplicity of presentation, we will assume that the values a^1, a^2, c^1, c^2 are known. Since $H'_\varepsilon(\varphi)$ is self-adjoint,[3] the optimality conditions for a minimizer of the functional $\mathcal{G}_{\varepsilon,\alpha}$ can be written in the form of the system of equations

$$\alpha(\Delta - I)(\phi_a - \phi_{a0}) = L^1_{\varepsilon,\alpha}(\phi_a, \phi_c)\,, \quad \alpha(\Delta - I)(\phi_c - \phi_{c0}) = L^2_{\varepsilon,\alpha}(\phi_a, \phi_c)\,, \text{ in } \Omega \tag{25a}$$

$$(\phi_a - \phi_{a0})_\nu = 0\,, \qquad (\phi_c - \phi_{c0})_\nu = 0\,, \text{ at } \Gamma \tag{25b}$$

where $\nu(x)$ is the external unit normal vector at $x \in \Gamma$, and

$$\begin{aligned} L^1_{\varepsilon,\alpha}(\phi_a, \phi_c) &= (a_1 - a_2)\, H'_\varepsilon(\phi_a) \left[\sum_{m=1}^{l} \left(\frac{\partial F_m(P_\varepsilon(\phi_a, \phi_c))}{\partial a}\right)^* (F_m(P_\varepsilon(\phi_a, \phi_c)) - h^\delta_m)\right] \\ &\quad -\alpha\beta_1 \left[H'_\varepsilon(\phi_a)\, \nabla\cdot\left(\frac{\nabla H_\varepsilon(\phi_a)}{|\nabla H_\varepsilon(\phi_a)|}\right)\right] \end{aligned} \tag{26a}$$

$$\begin{aligned} L^2_{\varepsilon,\alpha}(\phi_a, \phi_c) &= (c_1 - c_2)\, H'_\varepsilon(\phi_c) \left[\sum_{m=1}^{l} \left(\frac{\partial F_m(P_\varepsilon(\phi_a, \phi_c))}{\partial c}\right)^* (F_m(P_\varepsilon(\phi_a, \phi_c)) - h^\delta_m)\right] \\ &\quad -\alpha\beta_2 \left[H'_\varepsilon(\phi_c)\, \nabla\cdot\left(\frac{\nabla H_\varepsilon(\phi_c)}{|\nabla H_\varepsilon(\phi_c)|}\right)\right] \end{aligned} \tag{26b}$$

Note that, in order to implement the numerical algorithm for solving the optimal condition (26), we need to calculate the adjoint of the derivatives $\frac{\partial F_m}{\partial a}$ and $\frac{\partial F_m}{\partial a}$. Moreover, for any $\phi_a, \phi_c \in H^1(\Omega)$, the residual $F_m(P_\varepsilon(\phi_a, \phi_c)) - h^\delta_m \in L^2(\Gamma)$.

Remark 3. *Note that, if we define $(a_k, c_k) := P_\varepsilon(\phi^k_a, \phi^k_c)$, we have that $(a_k, c_k) \in D(F)$. We will use this fact in the next Lemma and in the level-set algorithm below.*

Remark 4. *Let $(a_k, c_k) \in \mathcal{D}(F)$ and $r^k_m \in L^2(\Gamma)$. Then,*

$$\left(\frac{\partial F_m}{\partial a}(a_k, c_k)\right)^* (r^k_m) = \nabla u^k_m \cdot \nabla w^k_m \tag{27}$$

and

$$\left(\frac{\partial F_m}{\partial c}(a_k, c_k)\right)^* (r^k_m) = -u^k_m\, w^k_m \tag{28}$$

where u^k_m and w^k_m are the unique solutions of the elliptic BVP of Neumann type

$$\begin{aligned} -\nabla(a_k \nabla u^k_m) + c_k u^k_m &= 0\,, \quad in \quad \Omega \\ a_k \frac{\partial u^k_m}{\partial \eta} &= g_m\,, \quad on \quad \Gamma\,, \end{aligned} \tag{29}$$

$$\begin{aligned} -\nabla(a_k \nabla w^k_m) + c_k w^k_m &= 0\,, \quad in \quad \Omega \\ a_k \frac{\partial w^k_m}{\partial \eta} &= r^k_m\,, \quad on \quad \Gamma\,, \end{aligned} \tag{30}$$

for $m = 1, \cdots, l$, respectively.

[3] Notice that $H'_\varepsilon(t) = \begin{cases} 1/\varepsilon & t \in (-\varepsilon, 0) \\ 0 & else \end{cases}$.

1. Evaluate the residual $[r_m]_{m=1}^l := [F_m(P_\varepsilon(\phi_a^k, \phi_c^k)) - h_m^\delta]_{m=1}^l = [u_s|_\Gamma - h_m^\delta]_{m=1}^l$, where $[u_s]_{m=1}^l \in [H^1(\Omega)]^l$ solves (29)

2. Evaluate $\left[\left(\frac{\partial F_m(P_\varepsilon(\phi_a,\phi_c))}{\partial a}\right)^* r_m\right]_{m=1}^l := [\nabla w_m \cdot \nabla u_m]_{m=1}^l \in [L^2(\Omega)]^l$, and $\left[\left(\frac{\partial F_m(P_\varepsilon(\phi_a,\phi_c))}{\partial c}\right)^* r_m\right]_{m=1}^l := -[w_m\, u_m]_{m=1}^l \in [L^2(\Omega)]^l$, where $[u_m]_{m=1}^l$ is the function computed in Step **1.** and $[w_m]_{m=1}^l \in [H^1(\Omega)]^l$ solves (30)

3. Calculate $L^1_{\varepsilon,\alpha}(\phi_a^k, \phi_c^k)$ and $L^2_{\varepsilon,\alpha}(\phi_a^k, \phi_c^k)$ as in (26).

4. Evaluate the updates $\delta\varphi$, $\delta\psi \in H^1(\Omega)$ by solving (25) and (25b)

5. Update the level set functions $\phi_a^{k+1} = \phi_a^k + \frac{1}{\alpha}\,\delta\phi_a^k$, $\phi_c^{k+1} = \phi_c^k + \frac{1}{\alpha}\,\delta\phi_c^k$.

Table 1: An explicit algorithm based on the iterative regularization method for solving the identification problem in diffusive optical tomography.

In the sequel we describe an explicit algorithm to implement the iterative regularization method for the coefficient identification problem (see Table 1). Each iteration of this algorithm consists of five steps:

- In the first step the residual vector $[r_m]_{j=s}^l \in [L^2(\Gamma)]^l$ corresponding to the iterate (ϕ_a^k, ϕ_c^k) is evaluated. This requires the solution of l elliptic BVP's given by (29).
- In the second step the solutions $[w_m]_{m=1}^l \in H^1(\Omega)$ of the adjoint problems for the residual components $[r_m]_{m=1}^l$ are evaluated. This corresponds to solving l elliptic BVP given by (30).
- The third step is the computation of adjoint of partial derivatives of F_m applied to the residual. It consist in to computing l scalar product and l inner-product in L^2 (namely $-[u_m\, w_m]_{m=1}^l$ and $[\nabla[w_m \cdot \nabla u_m]_{m=1}^l$.
- The fourth step consists in the computation of $L^1_{\varepsilon,\alpha}(\phi_a^k, \phi_c^k)$ and $L^2_{\varepsilon,\alpha}(\phi_a^k, \phi_c^k)$. Each computation requires the sum of l inner products in L^2.
- Finely, the updates $\delta\phi_a^k$, $\delta\phi_c^k \in H^1(\Omega)$ for the level-set functions ϕ_a^k and ϕ_c^k are evaluated. This corresponds to solving two non-coupled elliptic BVP's of Neumann type, namely (25) and (25b).

A similar algorithm was successfully used in [15, 8] to solve the inverse potential problem under the framework of level-sets and multiple level-sets respectively. However, what concerns the identification problem in diffusion optical tomography the method outlined above becomes disadvantageous if the number of physical experiments l in (11) is large. Indeed, in each iteration one has to solve $2l + 2$ elliptic BVP's.

5 Numerical Experiments

In this section we implement numerical algorithms based on the levelset approach derived in the previous sections for identifying the coefficient pair (a, c) in (1)-(2). The separate identification of the absorption coefficient c, based on either total or partial knowledge of a, is considered in Section 5.1. The separate identification of the diffusion coefficient a, based on either total or partial knowledge of c, is considered in Section 5.2. The simultaneous identification of the pair (a, c) is investigated in Section 5.3.

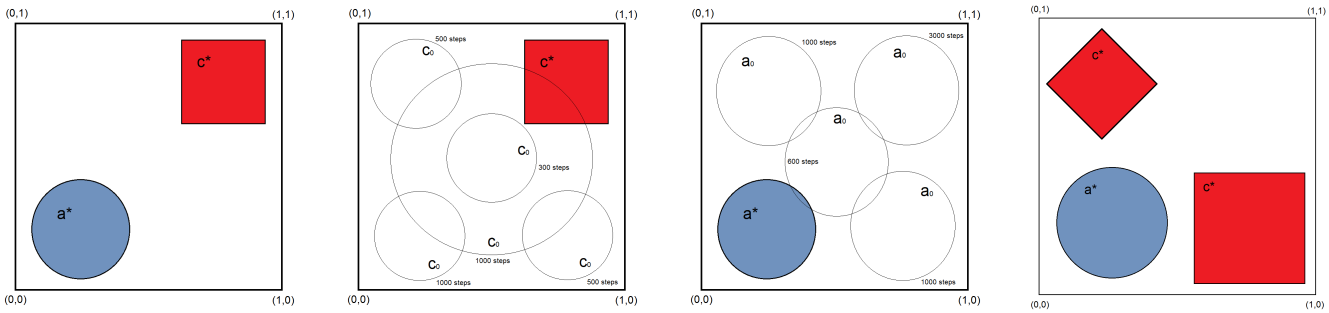

(a) (b) (c) (d)

Figure 1: **(a)** Exact coefficients for the first experiments in Sections 5.1 and 5.2. **(b)** Number of iterations needed for the identification of the absorption coefficient c^*, starting from distinct initial guesses c_0 (a^* is given; see Section 5.1). **(c)** Number of iterations needed for the identification of the diffusion coefficient a^*, starting from distinct initial guesses a_0 (c^* is given; see Section 5.2). **(d)** Exact coefficients for the second experiments in Sections 5.1 and 5.2.

5.1 Identification of the absorption coefficient

In what follows we consider the identification of the absorption coefficient c, based on either total or partial knowledge of a. In the first set of experiments, we consider problem (1)-(2) in the unit square with four sets ($l = 4$) of DtN experiments,[4] and exact solution (a^*, c^*) as shown in Figure 1 (a)

$$a^*(x) = \begin{cases} 10\,, & \text{inside blue inclusion} \\ 1\,, & \text{elsewhere} \end{cases}, \quad c^*(x) = \begin{cases} 10\,, & \text{inside red inclusion} \\ 0\,, & \text{elsewhere.} \end{cases}$$

As initial guess for the leveset method we choose distinct piecewise constant functions c_0, whose supports are depicted in Figure 1 (b). The constant values assumed by the exact solution c^* are assumed to be known, as well as the exact diffusion coefficient a^*. Moreover, exact data are used for the reconstruction (i.e., $\delta = 0$).

Thus, the inverse problem reduces to a shape identification problem for the absorption coefficient. Notice that, for each initial guess c_0 in Figure 1 (b), a corresponding number of steps is plotted. It stands for the number of iterations needed to compute an approximation of c^* (starting from the corresponding c_0) with a precision of 10^{-2} in the L^2-norm.

[4]Four distinct L^2-functions are used as Dirichlet boundary condition, in order to compute the corresponding Neumann data for the DtN operator. Each of these functions is supported at one of the four sides of $\partial\Omega$.

This experiment allow us to determine the computational effort necessary for the reconstruction of c^* w.r.t. distinct choices of c_0. **The identification problem for the absorption coefficient is known to be mildly ill-posed** [13, 20]. This fact is in agreement with the values plotted in Figure 1 (b), in the sense that the number of iterations necessary to achieve a good quality reconstruction **do not strongly oscillate** with the initial guess.

We conduct yet another experiment for identifying only the absorption coefficient. This time, we assume the exact solution of problem (1)-(2) to be given by the coefficient pair (a^*, c^*) in Figure 1 (d). The setup of the inverse problem remains the same (domain, available data, parameter to output operator, ...).

On the first run of the algorithm, see Figure 2 (a)–(c), the diffusion coefficient a^* is assumed to be exactly known. The levelset method is able to identify the absorption coefficient (see Figure 2 (a) for the evolution of the iteration error), and the iteration stagnates after that. The corresponding iteration errors for the initial guess c_0 and for the final iterate c_{5000} are plotted in pictures (b) and (c) respectively.

On the second run, see Figure 2 (d)–(f), we use the approximation $\bar{a}(x) \equiv 1$ for diffusion coefficient a^* and iterate to recover c^*. The levelset method is still able to identify the absorption coefficient, however with a poorer accuracy. Once again the iteration stagnates after the numerical convergence is reached (see Figure 2 (d) for the evolution of the iteration error). The corresponding iteration

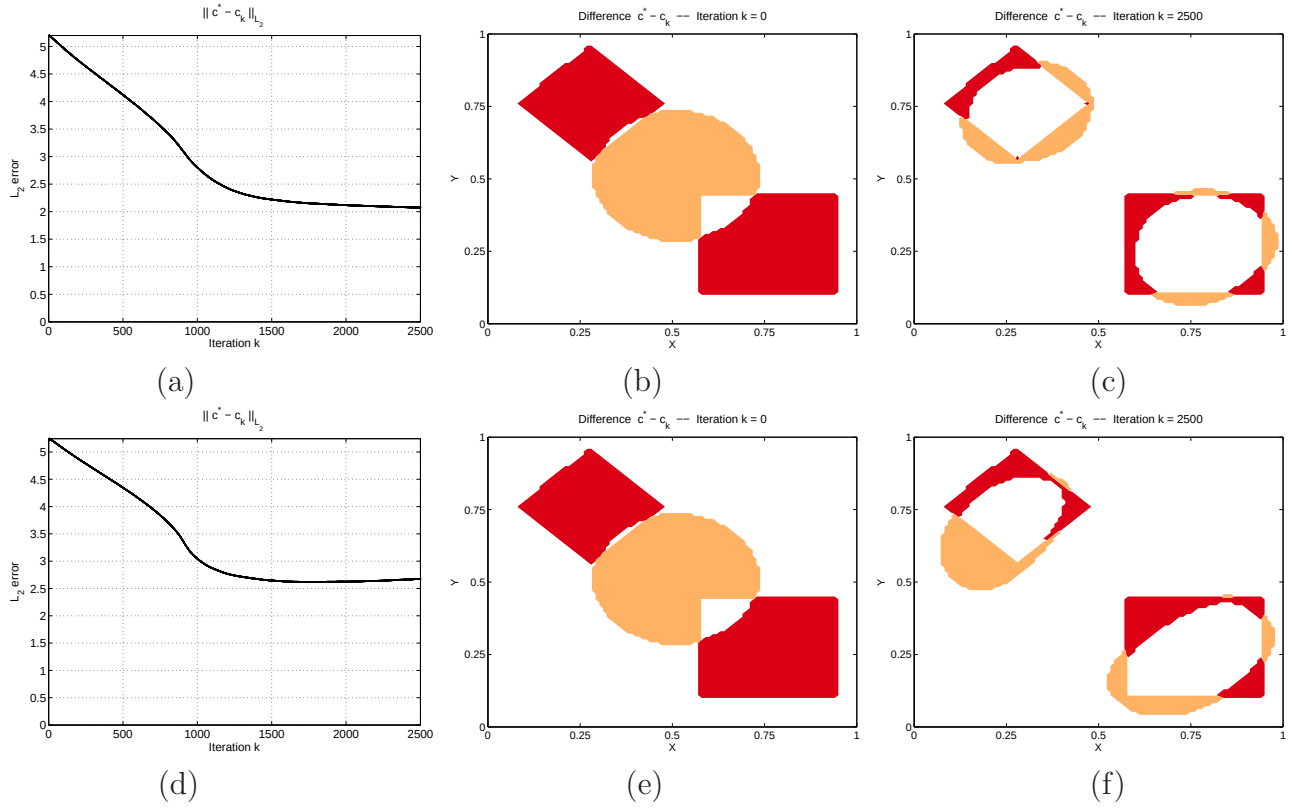

Figure 2: Section 5.1, 2nd example. **(a)**–**(c)** Identification of c^* from exact knowledge of a^*. **(a)** Evolution of the iteration error. **(b)** Difference between the initial guess c_0 and c^*. **(c)** Difference between c_{2500} and c^*. **(d)**–**(f)** Identification of c^* from partial knowledge of a^*. **(d)** Evolution of the iteration error. **(e)** Difference between the initial guess c_0 and c^*. **(f)** Difference between c_{2500} and c^*.

errors for the initial guess c_0 and for the final iterate c_{2500} are plotted in pictures (e) and (f) respectively.
Notice that the number of iteration steps needed to recover c^* (approximately 2000 in both runs) is much larger than in the previous experiment. This can be explained by the complexity of the geometry of the support of c^* in this experiment [15].

5.2 Identification of the diffusion coefficient

In what follows we consider the identification of the diffusion coefficient a, based on either total or partial knowledge of c. In the first set of experiments, we consider problem (1)-(2) in the unit square with four sets of DtN experiments, and the same exact solution (a^*, c^*) as in Section 5.1 (see Figure 1 (a)).

As initial guess for the levelset method we choose distinct piecewise constant functions a_0, whose supports are depicted in Figure 1 (c). Analogous as in Section 5.1, the constant values assumed by the exact solution a^* are assumed to be known, as well as the exact absorption coefficient c^*. Moreover, exact data are used for the reconstruction (i.e., $\delta = 0$).

This time, the inverse problem reduces to a shape identification problem for the diffusion coefficient. Once again we plot, for each initial guess a_0, a corresponding number of steps (see

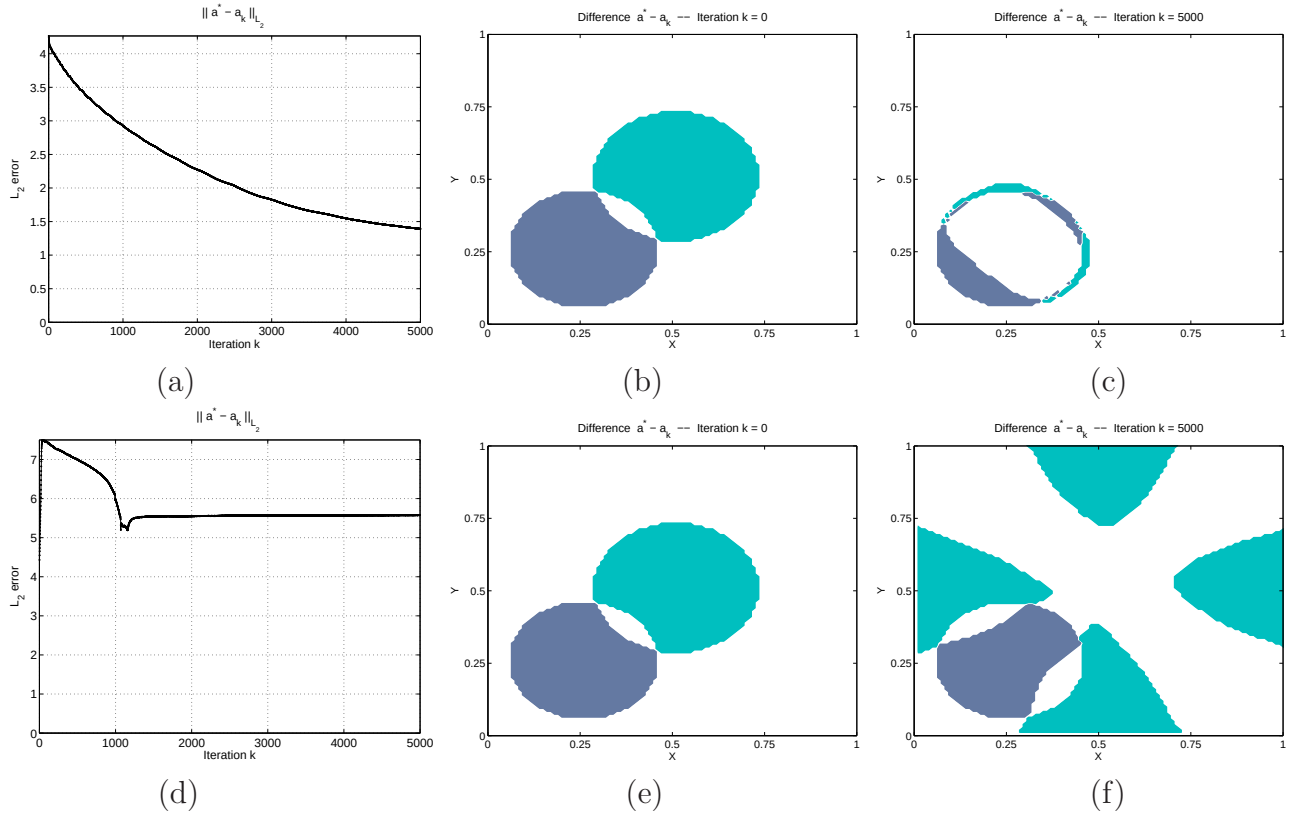

Figure 3: Section 5.2, 2nd example. **(a)**–**(c)** Identification of a^* from exact knowledge of c^*. **(a)** Evolution of the iteration error. **(b)** Difference between the initial guess a_0 and a^*. **(c)** Difference between a_{5000} and a^*. **(d)**–**(f)** Identification of a^* from partial knowledge of c^*. **(d)** Evolution of the iteration error. **(e)** Difference between the initial guess a_0 and a^*. **(f)** Difference between a_{5000} and a^*.

Figure 1 (c)). It stands for the number of iterations needed to compute an approximation of a^* (starting from the corresponding a_0) with a precision of 10^{-2} in the L^2-norm.

This experiment allow us to determine the computational effort necessary for the reconstruction of a^* w.r.t. distinct choices of a_0. **The identification problem for the diffusion coefficient is known to be exponentially ill-posed** [13, 19]. This fact is in agreement with the values ploted in Figure 1 (c), meanig that the number of iterations necessary to achieve a good quality reconstruction **does strongly oscilate** with the initial guess.

We conduct yet another experiment for identifying only the diffusion coefficient. This time, we assume the exact solution of problem (1)-(2) to be given by the coefficient pair (a^*, c^*) in Figure 1 (d). The setup of the inverse problem remains the same (domain, available data, parameter to output operator, ...).

On the first run of the algorithm, see Figure 3 (a)–(c), the absorption coefficient c^* is assumed to be exactly known. The levelset method is able to identify the diffusion coefficient (see Figure 3 (a) for the evolution of the iteration error), and the iteration stagnates after that. The corresponding iteration errors for the initial guess a_0 and for the final iterate a_{5000} are plotted in pictures (b) and (c) respectively.

On the second run, see Figure 3 (d)–(f), we use the approximation $\bar{c}(x) \equiv 1$ for the absorption coefficient c^* and iterate to recover a^*. The levelset method is no longer able to identify the diffusion coefficient. The iteration once again stagnates, this time at some configuration close to the initial guess (see Figure 3 (d) for the evolution of the iteration error). The corresponding iteration errors for the initial guess a_0 and for the final iterate a_{5000} are plotted in pictures (e) and (f) respectively.

5.3 Identification of both diffusion and absorption coefficients

In this last set of experiments we consider the levelset algorithm for the simultaneous identification of the coefficient pair (a, c) in (1), (2). Three examples are considered; the corresponding exact solutions are shown in Figure4. The setup of the inverse problem is the same as in Sections 5.1 and 5.2 (domain, available data, parameter to output operator, ...).

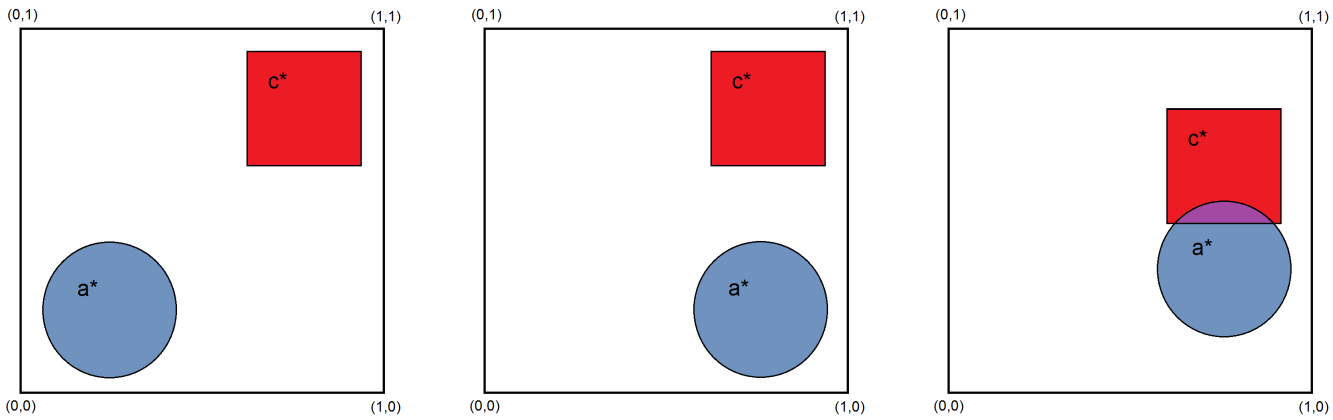

(a) (b) (c)

Figure 4: Section 5.3. **(a)–(c)** Exact solution for the first, second and third examples.

In the first example, the solution pair (a^*, c^*) is the one shown in Figure 4 (a). In order to devise an efficient iteration strategy for the simultaneous identification of both coefficients, we must take some facts into account:

F1) From the 2nd example in Section 5.1, we learn that the levelset method for identifying c^* performs well, even if a good approximation for a^* is not known (see Figure 2 (d)–(f)).

F2) On the other hand, from the 2nd example in Section 5.2, we learn that the levelset method for identifying a^* performs well if a good approximation for c^* is available, but may generate a sequence a_k that does not approximate a^* if $\|c_k - c^*\|$ is large.

F3) In the first run of the levelset algorithm for simultaneous identification of (a^*, c^*) we updated both coefficients (a_k, c_k) in every step, and observed that the iteration error $\|c_k - c^*\|$ decreases from the very first iteration. However, the iteration error $\|a_k - a^*\|$ only starts improving when $\|c_k - c^*\|$ is sufficiently small.

Thus, in order to save computational effort, we adopted the strategy to "freeze" the coefficient $a_k(x) = a_0(x) \equiv 1$ during the first iterations, and to iterate only w.r.t to c_k. We follow this strategy until the sequence c_k stagnates (this is an indication that the iteration error $\|c_k - c^*\|$ is small). In Figure 5 (a) and (e) this stage corresponds to the first $k_1 = 250$ iterative steps (notice that $\|a_k - a^*\|$ remains constant for $k = 0, \ldots, k_1$, while the difference $c_{k_1} - c^*$ is plotted in (g)).

After this first iteration stage, we freeze $c_k = c_{k_1}$ and iterate only w.r.t. a_k. This characterizes the second stage of the method. A natural question at this point would be: Why not to iterate with respect to both (a_k, c_k) for $k \geq k_1$? We tried to proceed this way, but what we observed is that: as long as $\|a_k - a^*\|$ does not significantly improve, the iterates c_k stagnate with $\|c_k - c_{k_1}\|$ almost constant.

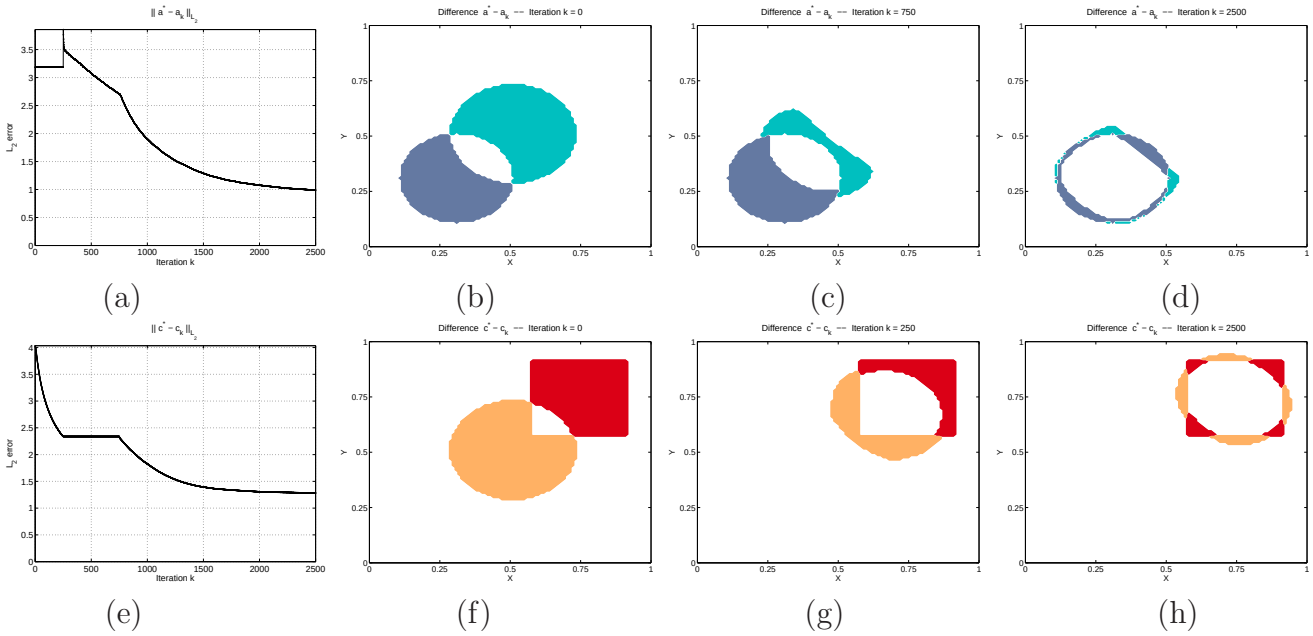

Figure 5: Section 5.3, 1st example. **(a)**–**(d)** Iterative reconstruction of a^*. **(a)** Evolution of the iteration error. **(b)** Difference $a_0 - a^*$. **(c)** Difference $a_{750} - a^*$. **(d)** Difference $a_{2500} - a^*$. **(e)**–**(h)** Iterative reconstruction of c^*. **(e)** Evolution of the iteration error. **(f)** Difference $c_0 - c^*$. **(g)** Difference $c_{250} - c^*$. **(h)** Difference $c_{2500} - c^*$.

This second stage of the iteration can be observed in Figure 5 (a) and (e). Notice that $\|a_k - a^*\|$ decreases significantly, while $\|c_k - c^*\|$ remains constant for $k = k_1, \ldots, k_2 = 750$ (the difference $a_{k_2} - a^*$ is plotted in (c)).

After the conclusion of the second iteration stage, the pair (a_k, c_k) is already a good approximation for (a^*, c^*) (see Figure 5 (c) and (g)). As a matter of fact, this approximation is so good that, proceeding with the iteration simultaneously w.r.t both (a_k, c_k), the iteration errors $\|a_k - a^*\|$ and $\|c_k - c^*\|$ are monotone decreasing. However, having in mind the convergence of the diffusion coefficient a_k to the correct solution a^* takes more iterations than the absorption coefficient c_k, in this third stage we decided that iteration step consist in one iteration w.r.t. the absorption coefficient c_k and two iterations w.r.t the diffusion coefficient a_k. (see Figure 5 (a) and (e) for $k \geq k_2$).

The introduction of this 3-stage iteration is motivated by the above mentioned facts (F1) – (F3). The calculation of optimal transition indexes k_1, k_2 between the three stages is a difficult task. However, since the degree of ill-posedness of the separate inverse problems for a and c is very distinct from each other it's not hard to get approximate values for k_1 and k_2 that will lead to a large gain in computational effort by using this 3-stage strategy.

The following second and third examples in this section do belong together. The corresponding exact solutions are shown in Figure 4 (b) and (c) respectively. Our goal is to investigate how the distance between the supports of components a^* and c^* of the exact solution pair may interfere with the quality of the reconstruction of each single coefficient. In the second example there is a positive distance between optimal , while in the third example both supports overlap.

Although the distance between supp(a^*) and supp(c^*) in example 2 is smaller than in example 1 above, the 3-stage iteration behaves similarly in both examples. The 1st-stage is ended after $k_1 =$

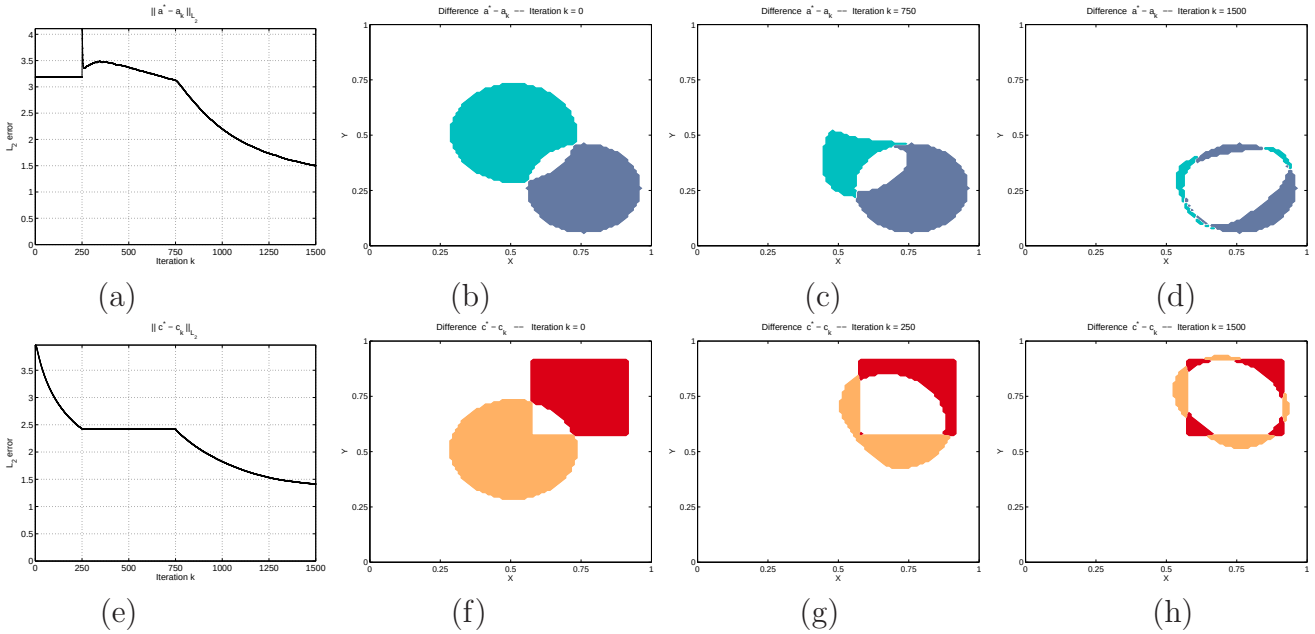

Figure 6: Section 5.3, 2nd example. **(a)**–**(d)** Iterative reconstruction of a^*. **(a)** Evolution of the iteration error. **(b)** Difference $a_0 - a^*$. **(c)** Difference $a_{750} - a^*$. **(d)** Difference $a_{1500} - a^*$. **(e)**–**(h)** Iterative reconstruction of c^*. **(e)** Evolution of the iteration error. **(f)** Difference $c_0 - c^*$. **(g)** Difference $c_{250} - c^*$. **(h)** Difference $c_{1500} - c^*$.

250 iterations, when the residual for the iterates c_k stagnate (see Figure 6 (g)). The 2nd-iteration stage corresponds to $k_1 \leq k \leq k_2 = 750$; the residual for the iterates a_k stagnate after k_2 steps (see Figure 6 (c)). The 3rd-stage of the iteration corresponds to $k \geq k_2$, where a substantial decrease in the iteration error $\|a_k - a^*\|$ can be observed (Figure 6 (a)), while $\|c_k - c^*\|$ decreases faster and stagnates after 2000 steps (Figure 6 (e)).

The third and last example reveled itself as the most difficult identification problem among all three considered in this section. The solution pair (a^*, c^*) is chosen such that the supports of a^* and c^* intersect (see Figure 4 (c)). We start the iteration once again keeping a_k constant during the first stage, until the residual stagnates with $k = k_1 = 250$. This part of the method is successful, since c_{k_1} delivers a good approximation for the solution c^* (Figure 4 (g)). For $k \geq k_1$ we start iterating w.r.t. a_k. This is the point where the difficulties arise. No matter how many iterations we compute w.r.t a_k, the approximation does not get better than the one plotted in Figure 4 (c), which is computed after $k_2 = 750$ steps (when the residual once again stagnates). For $k \geq k_2$ we have the configuration (a_k, c_k) shown in Figure 7 (c) and (g), and iterate further until the residual once more stagnates. After 1500 steps, no significant improvement can be observed in the iteration error (see Figure 7 (a) and (e)). The reconstruction of the absorption coefficient is very precise, but the obtained approximation for the diffusion coefficient is a poor one.

It is worth noticing that the poor reconstruction of a^* is not due to non-stable behaviour of our 3-stage algorithm. The particular exact solution (a^*, c^*) in this example (with intersecting supports) leads to a very hard identification problem. As a matter of fact, if we assume c^* to be known (as in Section 5.2) and try to identify only a^* in example 3 (starting from the same initial guess a_0), we experience exactly the same difficulty.

It is worth mentioning that all problems presented in this Section were solved using the standard levelset method described in Section 3.2, i.e., updating both (a_k, c_k) in every iterative step (and neglecting the 3-stage strategy). The final results of these iterations were the same as the ones presented here. However, the computational effort involved in the computation was by far much larger.

6 Conclusions

In this paper, we develop a level set regularization approach for simultaneous reconstruction of the piecewise constant coefficients (a, c) from a finite set of boundary measurements of optical tomography in the diffusive regime. From the theoretical point of view, we prove that the forward map F is continuous in the L^1-topology. Hence, follows the standard argumentation in previous papers of the authors (see [8]) we get that the proposed level set strategy is a regularization method. The main result behind the continuity of F is the generalization of Meyers Theorem for our case. On the other hand, given the acknowledgment acquired assuming that one of the two parameters is known, we propose a split strategy (that consist in frizzing $a = a_0$ and first iterate w.r.t. c until the iteration stagnate; then keep $c = c_k$ and start to iterate the level set approach w.r.t. a) for the simultaneous identification. Such strategy produces convergent results when a^* and c^* have no crossing sections. This strategy also reduces significatively the numerical computation effort.

The situation of non-convergence of the level set algorithm, i.e, when the solution (a^*, c^*)) have a crossing section (as in Subsection 5.3) is not a easy problem as was already reported in [27, 21, 3]. We conjecture that the level set algorithm will perform well if enough data (Newmann-Dirichlet pairs)

are available (remember that we shall have a uniqueness of identification under our assumptions [18]). However, we did not carefully explore this situation numerically. Since the numerical situation with many measurements is numerically demanding, a strategy like the one proposed in [23] become more appropriated. We let this problem for future and careful investigation.

Acknowledgments

A.D. acknowledges support from CNPq - Science Without Border grant 200815/2012-1, ARD-FAPERGS grant 0839 12-3 and CNPq grant 472154/2013-3.

The authors would like to thanks Prof. Dr. Uri M. Ascher for the discussions and suggestions.

7 Appendix

The main propose of this appendix is to show that under mild assumptions on the boundary (Neumann) data g, the solution u of (1), (2) belongs to $W^{1,p}(\Omega)$, for some $p > 2$ (therefore better than the standard regularity $u \in H^1(\Omega)$).

7.1 On the regularity of the solution of elliptic problems

As far as we know, this type of regularity, namely $u \in W^{1,p}(\Omega)$, goes back to pionering the work of Meyers [22], for elliptic BVPs with Dirichlet boundary conditions. Later on, Gallouet and

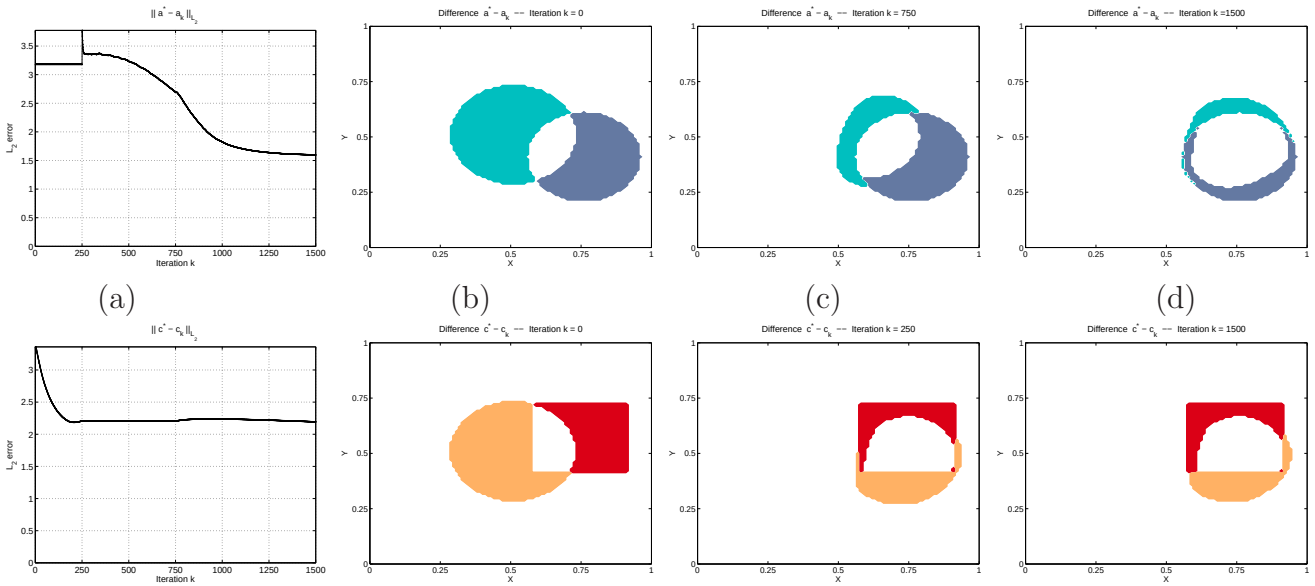

(a) (b) (c) (d)

(e) (f) (g) (h)

Figure 7: Section 5.3, 3rd example. **(a)**–**(d)** Iterative reconstruction of a^*. **(b)** Difference $a_0 - a^*$. **(c)** Difference $a_{750} - a^*$. **(d)** Difference $a_{1500} - a^*$. **(e)**–**(h)** Iterative reconstruction of c^*. **(f)** Difference $c_0 - c^*$. **(g)** Difference $c_{250} - c^*$. **(h)** Difference $c_{1500} - c^*$.

Monier [16] generalized Meyers' result to Neumann BVPs was presented. However, for the best of the authors acknowledgment there is no proves of such a result for the the solution u of (1)–(2).

In what follows, we show that: a) Meyers' theorem can be generalized for the problem Dirichlet (34)–(35); b) Gallouet and Monier's result can be generalized for the Neumann problem (34)–(35). The latter result in presented in Theorem 1, the proof follows the same outline of [16, Theorem 2].

We start by considering the (elliptic) boundary value problem (BVP):

$$-\nabla \cdot (A(x)\nabla u) = f \quad \text{in } \Omega \tag{31}$$

$$u = 0 \quad \text{on } \Gamma\,, \tag{32}$$

where $\Omega \subset \mathbb{R}^N$ is a bounded connected open set with boundary Γ Lipschitz, and the diffusion matrix $A(x) \in L^\infty(\Omega)^{N\times N}$ satisfies the following conditions for some $\alpha, \beta > 0$:

$$A(x)\xi \cdot \xi \geq \alpha|\xi|^2 \quad \text{(a.e.)} \quad \forall x \in \Omega \quad \forall \xi \in \mathbb{R}^N, \qquad \|A\|_\infty \leq \beta. \tag{33}$$

The following theorem is due to Meyers [22].

Theorem 6. *(Meyers) Let $\Omega \subset \mathbb{R}^N$ be a bounded connected open set of class $\mathcal{C}^2$ and let $\alpha, \beta > 0$. Then, there exists a real number $p_0 > 2$ (depending on Ω, α and β) such that the following condition hold for every $p \in [2, p_0)$:*

If $A(x)$ satisfies (33) and $f \in W^{-1,p}(\Omega)$, then the unique solution u of (31)– (32) belongs to $W_0^{1,p}(\Omega)$. Moreover, there exists a constant $C(p) > 0$ such that

$$\|u\|_{W_0^{1,p}} \leq C(p)\|f\|_{W^{-1,p}}.$$

Our goal now is to generalize Theorem 6 to the followsing class of BVPs:

$$-\nabla \cdot (A(x)\nabla u) + c(x)u = f \quad \text{in } \Omega \tag{34}$$

$$u = 0 \quad \text{on } \Gamma\,, \tag{35}$$

where $\Omega \subset \mathbb{R}^N$ satisfies the same assumptions of Theorem 6, $N \in \{2, 3, 4\}$, the diffusion matrix $A(x)$ satisfies (33) (for some $\alpha, \beta > 0$) and $c(x)$ is real-valued measurable function satisfying the following condition:

$$0 < \underline{c} \leq c(x) \leq \overline{c} \quad \text{a.e.} \quad \forall x \in \Omega, \tag{36}$$

for some $0 < \underline{c} \leq \overline{c}$.

Proposition 7. *Let $\Omega \subset \mathbb{R}^N$ be a bounded connected open set of class $\mathcal{C}^2$, where $N \in \{2, 3, 4\}$. Let also $\alpha, \beta > 0$ and $0 < \underline{c} \leq \overline{c}$. Then, there exists a real number $p_0 > 2$ (depending only on Ω, α and β) such that the following condition hold for every $p \in (2, p_0)$:*

If $A(x)$ and $c(x)$ satisfy (33) and (36), respectively, and $f \in W^{-1,p}(\Omega)$, then the unique solution u of (34)– (35) belongs to $W_0^{1,p}(\Omega)$.

Proof. Let $p_0 > 2$ be the real number given by Theorem 6 (which depends only on Ω, α and β). Take $p \in (2, p_0)$, let $q := p/(p-1)$ be its conjugate and assume that $f \in W^{-1,p}(\Omega) = W_0^{1,q}(\Omega)'$, and

that $A(x)$ and $c(x)$ satisfy (33) and (36), respectively. We know, in this case, from the Lax-Milgram Theorem, that the unique solution $u \in H^1(\Omega)$ of (34)–(35) satisfies

$$\int_\Omega A(x)\nabla u \nabla \varphi dx + \int_\Omega c(x)u\varphi dx = \langle f, \varphi\rangle_{H^{-1}\times H_0^1} \qquad \forall \varphi \in H_0^1(\Omega). \tag{37}$$

Define $\tilde{f} : W_0^{1,q}(\Omega) \to \mathbb{R}$ by

$$\langle \tilde{f}, \varphi\rangle := \langle f, \varphi\rangle_{H^{-1}\times H_0^1} - \int_\Omega c(x)u\varphi dx \qquad \forall \varphi \in W_0^{1,q}(\Omega). \tag{38}$$

Since $f \in W^{-1,p}(\Omega)$, it follows that $\langle f, \varphi\rangle_{H^{-1}\times H_0^1}$ is well-defined for every $\varphi \in W_0^{1,q}(\Omega)$. In what follows, we shall prove that the map $h : \varphi \mapsto \int_\Omega c(x)u\varphi dx$ is also well-defined for every $\varphi \in W_0^{1,q}(\Omega)$ and belongs to $W^{-1,p}(\Omega)$. To this end, consider first the case $N = 2$. In this case, since $q < 2$, we have the continuous embedding [4, Corollary 9.14] $W_0^{1,q}(\Omega) \hookrightarrow W^{1,q}(\Omega) \hookrightarrow L^{q^*}(\Omega)$, where $q^* = 2q/(2-q) > 2$. Letting $s := q^*/(q^*-1)$ be the conjugate of q^* we have $s < 2$ (because $q^* > 2$) and, as a consequence, the continuous embedding [4] $H_0^1(\Omega) \hookrightarrow L^2(\Omega) \hookrightarrow L^s(\Omega)$. Using the latter inclusions, the fact that $u \in H_0^1(\Omega)$, condition (36) and the Holder inequality, we obtain (for all $\varphi \in W_0^{1,q}(\Omega)$):

$$\begin{aligned} |\langle h, \varphi\rangle| = \left|\int_\Omega c(x)u\varphi dx\right| &\le \overline{c}\|u\|_{L^s}\|\varphi\|_{L^{q^*}} \\ &\le \overline{c}\|u\|_{L^s}\|\varphi\|_{W_0^{1,q}}, \end{aligned} \tag{39}$$

which proves that $h \in W^{-1,p}(\Omega)$. Consider now the case $N \in \{3, 4\}$ and let $q^* := qN/(N-q) > 1$ and (as before) $s := q^*/(q^*-1)$ its conjugate. In this case, we have also the continuous embeddings [4, Corollary 9.14] $W_0^{1,q}(\Omega) \hookrightarrow W^{1,q}(\Omega) \hookrightarrow L^{q^*}(\Omega)$ and, since $1 \le s \le 2^* := 2N/(N-2)$, $H_0^1(\Omega) \hookrightarrow H^1(\Omega) \hookrightarrow L^s(\Omega)$. Using the same reasoning as in the case $N = 2$ we find that (39) also holds when $N \in \{3, 4\}$, which in turn proves that $\tilde{f}$ is well-defined and belongs to $W^{-1,p}(\Omega)$. Using the latter fact, conditions (37) and (38) and the definition of h we obtain that u satisfy

$$\int_\Omega A(x)\nabla u \nabla \varphi dx = \langle \tilde{f}, \varphi\rangle_{H^{-1}\times H_0^1} \qquad \forall \varphi \in H_0^1(\Omega), \tag{40}$$

where $\tilde{f} = f - h \in W^{-1,p}$, i.e., u is a solution of (31)–(32) with $f = \tilde{f}$ given by (38). The result now follows as a direc application of Theorem 6 to $A(x)$ and $\tilde{f}$. □

We note that, unlike Theorem 6, in Proposition 7 we have $2 \le N \le 4$ and $p > 2$. Moreover, the scalar $p_0 > 2$ depends only on Ω, α and β and no longer depends on $\overline{c}$ and $\underline{c}$.

Consider now the BVP (1)-(2), where $\Omega \subset \mathbb{R}^N$ satisfies the same assumption as in (31)–(32), $N \in \{2, 3, 4\}$, and the diffusion and absorption coefficients $(a(x), c(x)) \in D(F)$. Then, we are ready to present a proof for Theorem 1.

Proof of Theorem 1 The proof presented here follows the same outline of [16, Theorem 2]. We will skip some details of the proof that are analogues to the ones presented in the latter reference, whenever we fell that clarity is not sacrificed. It follows from [16, Proposition 1] that there exits a

family $\{U_i\}_{i=0}^k$ of open sets in $\mathbb{R}^N$ satisfying $\overline{U_0} \subset \Omega$, $\overline{\Omega} \subset \bigcup_{i=0}^k U_i$, and a family of homeomorphisms $J_i : U_i \to B$ sucht that (for all $i = 1, \cdots, k$) J_i and $H_i := J_i^{-1}$ are Lipscthitz continuous and $J_i(\Omega \cap U_i) = B_+$ and $J_i(\Gamma \cap U_i) = B^{N-1}$, where $B := \{x \in \mathbb{R}^N \,|\, |x| < 1\}$, $B_+ := B \cap \{(x', x_N) \,|\, x' \in \mathbb{R}^{N-1}, x_N > 0\}$ and $B^{N-1} := B \cap \{(x', 0) \,|\, x' \in \mathbb{R}^{N-1}\}$.

For $2 < p < 2^* := 2N/(N-2)$, $q := p/(p-1)$ and $g \in W^{1-(1/q),q}(\Gamma)'$, let $u := u(a, c)$ be the (weak) solution of (1)–(2), for some pair $(a, c) \in D(F)$. We know that u satisfies (6) (The existence of such u is given by the Lax-Milgram theorem and the definition of $D(F)$).

Step 1: Localization. Let $\{\theta_i\}_{i=1}^k$ be a partition of unity associated to the family of open sets $\{U_i\}_{i=1}^k$. For each $i \in \{1, \cdots, k\}$, define

$$u_i = \theta_i u.$$

Since u satisfies (6), it follows that u_i satisfies (for all $i = 0, \cdots, k$)

$$\int_\Omega a(x)\nabla u_i \nabla \varphi dx + \int_\Omega c(x) u_i \varphi dx = \int_\Omega a(x)\nabla\theta_i[u\nabla\varphi - \nabla u\varphi]dx + \int_\Gamma (\theta_i\varphi) g d\sigma \quad \forall \varphi \in H^1(\Omega). \tag{41}$$

For $\varphi \in H^1(\Omega)$ and $i \in \{0, \cdots, k\}$, consider a function $\gamma \in C^\infty(\mathbb{R}^N)$ such that $\operatorname{supp}(\theta_i) \subset \operatorname{supp}(\gamma) \subset U_i$ and $\gamma(x) = 1$ for all $x \in \operatorname{supp}(\theta_i)$. Direct calculations yields

$$\begin{aligned}\int_\Omega a(x)\nabla u_i \nabla(\gamma\varphi)dx + \int_\Omega c(x)u_i\gamma\varphi dx &= \int_{\Omega\cap\operatorname{supp}(\theta_i)} a(x)\nabla u_i\nabla\varphi dx + \int_{\Omega\cap\operatorname{supp}(\theta_i)} c(x)u_i\varphi dx \\ &= \int_{\Omega\cap U_i} a(x)\nabla u_i\nabla\varphi dx + \int_{\Omega\cap U_i} c(x)u_i\varphi dx.\end{aligned}$$

Combining the latter identity with (41) for $\gamma\varphi$ in the place of φ, we obtain the following identity for all $i = 0, \cdots, k$ and $\varphi \in H^1(\Omega \cap U_i)$,

$$\begin{aligned}\int_{\Omega\cap U_i} a(x)\nabla u_i\nabla\varphi dx + \int_{\Omega\cap U_i} c(x)u_i\varphi dx &= \int_\Omega a(x)\nabla\theta_i[u\nabla(\gamma\varphi) - (\gamma\varphi)\nabla u]dx + \int_\Gamma (\theta_i\gamma\varphi)gd\sigma \\ &:= \langle f_i, \varphi\rangle_{H^1(\Omega\cap U_i)'\times H^1(\Omega\cap U_i)},\end{aligned} \tag{42}$$

where $\gamma\varphi$ is extended by zero on Ω. Since $p < 2^*$, it follows from the Sobolev embedding theorem that $f_i \in W^{1,q}(\Omega \cap U_i)'$ for all $i = 0, \cdots, k$.

Step 2: Interior estimates. Let B_R be a open ball with radius $R > 0$ such that $U_0 \subset B_R$. Extending u_0 by zero outside U_0 and noting that $f_0 \in W^{-1,p}(B_R)$, we conclude from (42) that $u_0 \in H_0^1(B_R)$ satisfies the following condition:

$$\int_{B_R} a(x)\nabla u_0\nabla\varphi dx + \int_{B_R} c(x)u_0\varphi dx = \langle f_0, \varphi\rangle_{H^1(B_R)'\times H^1(B_R)} \quad \forall \varphi \in H_0^1(B_R) \tag{43}$$

$$u_0 = 0, \quad \text{on } \partial B_R. \tag{44}$$

Thus, using Proposition 7 for $\Omega = B_R$, $\alpha = \underline{a}$, $\beta = \overline{a}$, $A = a$ and $f = f_0$ we conclude that there exists $p_0 > 2$ such that $u_0 \in W^{-1,p}(B_R)$ whenever $p \in (2, p_0)$ (we can assume that $p_0 < 2^*$).

Step 3: Estimates near the boundary. Fix $i \in \{0, \cdots, k\}$, define $v = u_i$ and denote $f = f_i$, $U = U_i$, $J = J_i$, etc. In this case, (42) becomes

$$\int_{\Omega\cap U} a(x)\nabla v\nabla\varphi dx + \int_{\Omega\cap U} c(x)v\varphi dx = \langle f, \varphi\rangle_{H^1(\Omega\cap U)'\times H^1(\Omega\cap U)} \quad \forall \varphi \in H^1(\Omega \cap U). \tag{45}$$

Defining $w = v \circ H$, $y = Jx$ (for all $x \in \Omega \cap U$) we have $v = w \circ J$ and $x = Hy$ (for all $y \in B_+$). For $\psi \in H^1(B_+)$ define also $\varphi = \psi \circ J$. Direct calculations yields the following identities, for all $\forall x \in \Omega \cap U$:

(a) $\nabla v(x) = \nabla J(x)^T \nabla w(Jx)$;

(b) $\nabla \varphi(x) = \nabla J(x)^T \nabla \psi(Jx)$;

(c) $a(x)\nabla v(x)\nabla \varphi(x) = \nabla J(x) a(x) \nabla J(x)^T \nabla w(Jx) \cdot \nabla \psi(Jx)$.

Using (a), (b), (c) and the formulae of change of variables, we find

$$\int_{\Omega \cap U} a(x)\nabla v(x) \cdot \nabla \varphi(x) dx = \int_{B_+} \Lambda(y) \nabla w(y) \cdot \nabla \psi(y) dy, \tag{46}$$

and

$$\int_{\Omega \cap U} c(x) v(x) \varphi(x) dx = \int_{B_+} C(y) w(y) \psi(y) dy, \tag{47}$$

where

$$\Lambda(y) := a(Hy) |\det \nabla H(y)| \nabla J(Hy) \nabla J(Hy)^T, \qquad C(y) := c(Hy) |\det \nabla H(y)| \quad \forall y \in B_+. \tag{48}$$

Since $H = J^{-1}$ is Lipschitz continuous, it follows that $\nabla H(y)$ (which is defined almost everywhere) and $\det \nabla H(y)$ are uniformly bounded. Therefore, using (**??**), we conclude that there exist $\alpha', \beta' > 0$ and $0 < \underline{C} \leq \overline{C}$ such that

$$\Lambda(y)\xi \cdot \xi \geq \alpha' |\xi|^2 \quad \left(\forall \text{ a.e. } y \in B_+, \ \forall \xi \in \mathbb{R}^N\right), \quad \|\Lambda\|_\infty \leq \beta', \quad 0 < \underline{C} \leq C(y) \leq \overline{C} \quad \forall \text{ a.e. } y \in B_+. \tag{49}$$

Now, let us look at the right hand side of (45). Since $f \in W^{1,q}(\Omega \cap U)'$, it follows from the Riez Representation Theorem that there exist $\tilde{f} \in L^p(\Omega \cap U)$ and $F \in L^p(\Omega \cap U)^N$ such that

$$\langle f, \phi \rangle_{W^{1,q}(\Omega \cap U)' \times W^{1,q}(\Omega \cap U)} = \int_{\Omega \cap U} \tilde{f} \phi dx + \int_{\Omega \cap U} F(x) \cdot \nabla \phi(x) dx \quad \forall \phi \in W^{1,q}(\Omega \cap U). \tag{50}$$

Using the latter identity, (b) and the formulae of change of variables, we obtain for $\psi \in H^1(B_+)$ (recall that $\varphi = \psi \circ J$):

$$\begin{aligned} \langle f, \varphi \rangle_{W^{1,q}(\Omega \cap U)' \times W^{1,q}(\Omega \cap U)} &= \int_{B_+} \tilde{f}(Hy) |\det \nabla H(y)| \psi(y) dy + \int_{B_+} |\det \nabla H(y)| \nabla J(Hy) F(Hy) \cdot \nabla \psi(y) dy \\ &=: \langle h, \psi \rangle_{H^1(B_+)' \times H^1(B_+)}, \end{aligned} \tag{51}$$

where $h \in W^{1,q}(B_+)'$. It follows from (45)–(47) and the latter idendity that w satisfies the following conditions:

$$\begin{aligned} &w \in H^1(B_+), \\ &\int_{B_+} \Lambda(y) \nabla w(y) \cdot \nabla \psi(y) dy + \int_{B_+} C(y) w(y) \psi(y) dy = \langle h, \psi \rangle_{H^1(B_+)' \times H^1(B_+)} \quad \forall \psi \in H^1(B_+). \end{aligned} \tag{52}$$

Step 3a: Extention of $w(y)$ and h. The funcion $w(y)$ and the functional h are extended by reflection. Let $w^* \in H_0^1(B)$ and $h^* \in W^{-1,p}(B)$ be defined, respectively, by

$$w^*(x', x_N) = \begin{cases} w(x', x_N), & \text{if} \quad x_N \geq 0 \\ w(x', -x_N), & \text{if} \quad x_N < 0, \end{cases} \tag{53}$$

and

$$\langle h^*, \phi \rangle_{W^{1,q}(B)' \times W^{1,q}(B)} = \langle h, \phi \rangle_{W^{1,q}(B_+)' \times W^{1,q}(B_+)} + \langle h, \phi(x', -x_N) \rangle_{W^{1,q}(B_+)' \times W^{1,q}(B_+)} \quad \forall \phi \in W^{1,q}(B). \tag{54}$$

Step 3b: Extension of $\Lambda(y)$ and $C(y)$. Denote $\Lambda(y) = (\alpha_{i,j}(y))$ for $y \in B_+$, where $\Lambda(y)$ is defined in (48), and define $\Lambda^*(x) = (\alpha^*_{i,j}(x))$ (for $x = (x', x_N) \in B$) as follows:

$$\alpha^*_{i,j}(x) = \begin{cases} \alpha_{i,j}(x) \quad \text{if} \quad x_N \geq 0, \\ \alpha_{i,j}(x', -x_N) \quad \text{if} \quad i, j < N-1 \text{ and } x_N < 0, \\ -\alpha_{i,j}(x', -x_N) \quad \text{if} \quad i = N \text{ or } j = N \text{ but } (i,j) \neq (N,N), \text{ and } x_N < 0, \\ \alpha_{N,N}(x', -x_N) \quad \text{if} \quad i = j = N \text{ and } x_N < 0. \end{cases} \tag{55}$$

Using the above definition of $\Lambda^*(y)$ and (53) we have that

$$\int_{B_-} \Lambda^*(x) \nabla w^*(x) \cdot \nabla \phi(x) dx = \int_{B_+} \Lambda(y) \nabla w(y) \cdot \nabla \phi(y', -y_N) dy \quad \forall \phi \in H^1(B), \tag{56}$$

where $B_- := \{x = (x', x_N) \in B \,|\, x_N \leq 0\}$.

Analogously to $w(y)$, the coeffient $C(y)$ is also extended to B by reflection. Define for all $x = (x', x_N) \in B$:

$$C^*(x) = \begin{cases} C(x) \quad \text{if} \quad x_N \geq 0, \\ C(x', -x_N) \quad \text{if} \quad x_N < 0. \end{cases} \tag{57}$$

It follows from (48), (49) and from the definitions of $\Lambda^*(x)$ and $C^*(x)$ that there exist $\alpha^*, \beta^* > 0$ and $0 < \underline{C^*} \leq \overline{C^*}$ such that

$$\Lambda^*(x)\xi \cdot \xi \geq \alpha^* |\xi|^2 \quad \left(\forall \text{ a.e. } x \in B, \ \forall \xi \in \mathbb{R}^N\right), \quad \|\Lambda^*\|_\infty \leq \beta^*, \quad 0 < \underline{C^*} \leq C(x) \leq \overline{C^*} \quad \forall \text{ a.e. } x \in B. \tag{58}$$

Step 4: Conclusion. Using the latter facts in Step 3, one can show that

$$\begin{aligned} \int_{B_-} C^*(x) w^*(x) \phi(x) dx &= \int_{B_-} C(x', -x_N) w(x', -x_N) \phi(x', x_N) dx \\ &= \int_{B_+} C(y) w(y) \phi(y', -y_N) dy \quad \forall \phi \in H^1(B). \end{aligned} \tag{59}$$

From (53)–(59), we find

$$\begin{aligned}\int_B \Lambda^*(x)\nabla w^*(x)\nabla\phi(x)dx + \int_B C^*(x)w^*(x)\phi(x)dx &= \int_{B_+} \Lambda(y)\nabla w(y)[\nabla\phi(y) + \nabla\phi(y', -y_N)]dy \\ &+ \int_{B_+} C(y)[\phi(y) + \phi(y', -y_N)]dy \\ &= \langle h, \phi(y) + \phi(y', -y_N)\rangle_{H^1(B_+)'\times H^1(B_+)} \\ &= \langle h^*, \phi\rangle_{H^1(B)'\times H^1(B)} \quad \forall\phi \in H_0^1(B).\end{aligned}$$

The latter identity proves that $w^* \in H_0^1(B)$ is the (unique) solution of the problem

$$-\nabla\cdot(\Lambda^*(x)\nabla w^*) + C^*(x)w^* = h^* \quad \text{in } B \tag{60}$$

$$w^* = 0 \quad \text{on } \partial B. \tag{61}$$

Let $2 < p_i < 2^*$ (recall that $i \in \{0, 1, \cdots, k\}$ is fixed in Step 3) be given by Proposition 7 (for $\Omega = B$, $\alpha = \alpha^*$ and $\beta = \beta^*$). Assuming that $p \in (2, p_i)$ and using the latter theorem with $A = \Lambda^*$, $c = C^*$ and $f = h^*$, we conclude that w^* belongs to $W_0^{1,p}(B)$. Using a restriction argument we conclude that $v = u_i \in W_0^{1,p}(\Omega)$ for all $i \in \{0, \cdots, k\}$ and $2 < p < p_M := \min_{i=0,\cdots,k} p_i$. The desired regularity result for u follows from the latter inclusion and from the fact that $u = \sum_{i=0}^k u_i$.

References

[1] S. R. Arridge. Optical tomography in medical imaging. *Inverse Problems*, 15(2):R41–R93, 1999.

[2] S. R. Arridge and W.R.B. Lionheart. Nonuniqueness in diffusion-based optical tomography. *Opt. Lett.*, 23:882–4, 1998.

[3] S. R. Arridge and M. Schweiger. A general framework for iterative reconstruction algorithms in optical tomography, using a finite element method. In *Computational radiology and imaging (Minneapolis, MN, 1997)*, volume 110 of *IMA Vol. Math. Appl.*, pages 45–70. Springer, New York, 1999.

[4] Haim Brezis. *Functional analysis, Sobolev spaces and partial differential equations*. Universitext. Springer, New York, 2011.

[5] M. Burger and S. Osher. A survey on level set methods for inverse problems and optimal design. *European J. Appl. Math.*, 16(2):263–301, 2005.

[6] R. Dautray and J.-L. Lions. *Mathematical analysis and numerical methods for science and technology. Vol. 2*. Springer-Verlag, Berlin, 1988.

[7] A. De Cezaro, A. Leitão, and X.-C. Tai. On level-set type methods for recovering piecewise constant solutions of ill-posed problems. In X.-C. Tai, K. Mørken, K. Lysaker, and K.-A. Lie, editors, *Scale Space and Variational Methods in Computer Vision*, volume 5667 of *Lecture Notes in Comput. Sci.*, pages 50–62. Springer, Berlin, 2009.

[8] A. De Cezaro, A. Leitão, and X.-C. Tai. On multiple level-set regularization methods for inverse problems. *Inverse Problems*, 25:035004, 2009.

[9] A. De Cezaro, A. Leitão, and X.-C. Tai. On piecewise constant level-set (pcls) methods for the identication of discontinuous parameters in ill-posed problems. *Inverse Problems*, 29:015003, 2013.

[10] A. De Cezaro and A. Leitão. Level-set of L^2type for recovering shape and contrast in inverse problems. *Inverse Problems in Science and Enginnering*, 20(4):517–587, 2012.

[11] A. De Cezaro and A. Leitão. Corrigendum: Level-set of L^2type for recovering shape and contrast in inverse problems. *Inverse Problems in Science and Enginnering*, 21:1–2, 2013.

[12] O. Dorn and D. Lesselier. Level set methods for inverse scattering—some recent developments. *Inverse Problems*, 25(12):125001, 11, 2009.

[13] H. W. Engl, M. Hanke, and A. Neubauer. *Regularization of inverse problems*, volume 375 of *Mathematics and its Applications*. Kluwer Academic Publishers Group, Dordrecht, 1996.

[14] L.C. Evans and R.F. Gariepy. *Measure theory and fine properties of functions*. Studies in Advanced Mathematics. CRC Press, Boca Raton, FL, 1992.

[15] F. Frühauf, O. Scherzer, and A. Leitão. Analysis of regularization methods for the solution of ill-posed problems involving discontinuous operators. *SIAM J. Numer. Anal.*, 43:767–786, 2005.

[16] T. Gallouet and A. Monier. On the regularity of solutions to elliptic equations. *Rend. Mat. Appl. (7)*, 19(4):471–488 (2000), 1999.

[17] A. P. Gibson, J. C. Hebden, and S. R. Arridge. Recent advances in diffuse optical imaging. *Physics in Medicine and Biology*, 50(4):R1–R43, 2005.

[18] B. Harrach. On uniqueness in diffuse optical tomography. *Inverse Problems*, 25(5):055010, 14, 2009.

[19] V. Isakov. *Inverse problems for partial differential equations*, volume 127 of *Applied Mathematical Sciences*. Springer, New York, second edition, 2006.

[20] B. Kaltenbacher, A. Neubauer, and O. Scherzer. *Iterative regularization methods for nonlinear ill-posed problems*, volume 6 of *Radon Series on Computational and Applied Mathematics*. Walter de Gruyter GmbH & Co. KG, Berlin, 2008.

[21] V. Kolehmainen, S. R. Arridge, W. R. B. Lionheart, M. Vauhkonen, and J. P. Kaipio. Recovery of region boundaries of piecewise constant coefficients of an elliptic PDE from boundary data. *Inverse Problems*, 15(5):1375–1391, 1999.

[22] N. G. Meyers. An L^p-estimate for the gradient of solutions of second order elliptic divergence equations. *Ann. Scuola Norm. Sup. Pisa (3)*, 17:189–206, 1963.

[23] F. Roosta-Khorasani, Kees van den Doel, and Uri M. Ascher. Stochastic algorithms for inverse problems involving pdes and many measurements. *SIAM J. Scient. Comput.*, 36:s3–s22, 2014.

[24] F. Santosa. A level-set approach for inverse problems involving obstacles. *ESAIM Contrôle Optim. Calc. Var.*, 1:17–33, 1995/96.

[25] T. Tarvainen, B.T. Cox, J.P. Kaipo, and S.R. Arridge. Reconstructing absorption and scattering distributions in quantitative photoacoustic tomography. *Inverse Problems*, 28:084009, 2012.

[26] K. van den Doel and U. M. Ascher. On level set regularization for highly ill-posed distributed parameter estimation problems. *J. Comput. Phys.*, 216(2):707–723, 2006.

[27] Yong Xu, Xuejun Gu, Taufiquar Khan, and Huabei Jiang. Absorption and scattering images of heterogeneous scattering media can be simultaneously reconstructed by use of dc data. *Appl. Opt.*, 41(25):5427–5437, 2002.

[28] A. D. Zacharopoulos, S.R. Arridge, O. Dorn, V. Kolehmainen, and J. Sikora. Three-dimensional reconstruction of shape and piecewise constant region values for optical tomography using spherical harmonic parametrization and a boundary element method. *Inverse Problems*, 22(5):1509–1532, 2006.